

MAGNETIC CIRCULAR ANISOTROPY IN CRYSTALS

N. V. STAROSTIN and P. P. FEOFILOV

Usp. Fiz. Nauk 97, 621-655 (April, 1969)

I. INTRODUCTION

IN the study of the energy and crystal-chemical structure of solids, modern spectroscopy resorts more and more frequently to methods involving investigations in external fields—electric or magnetic—and under conditions of directed deformation. A distinct place among these methods is occupied by investigations in a magnetic field. The distinguishing feature of these methods is that the influence of the magnetic field on the system cannot be described by assigning an ordinary (polar) field-intensity vector, as in the case of the electric field. It can be characterized by specifying a current-carrying circuit, which is equivalent to specifying an axial vector. As a result, besides the ordinary optical anisotropy, which always occurs in a medium under the influence of external fields and deformations (birefringence effects), an additional circular anisotropy appears in a magnetic field and is connected with the non-equivalence of the two rotation directions in a plane perpendicular to the field.

In anisotropic crystals, at an arbitrary direction of the wave vector, the magnetic field influences the propagation of the light relatively little, causing only the appearance of a weak (additional) ellipticity of the oscillations. The relative changes of the components of the dielectric tensor under ordinary experimental conditions amounts to approximately 10^{-4} , and phenomena of double magnetic refraction are usually not observed against the background of natural birefringence.

Exceptions in this respect are the directions of the optical axes, along which a unique degeneracy takes place in the absence of external fields, namely two states of polarization correspond here to the same refractive index n and to the same absorption coefficient k . In this connection, particular interest attaches to an investigation of magneto-optical phenomena in optically isotropic cubic crystals, where there are no complications connected with the intrinsic anisotropy and the phenomena can be observed in pure form. An external magnetic field lifts in such cases the degeneracy of the two states of circular polarization for each propagation direction, and the values of n and k become different for right- and left-polarized light. This leads to a number of magneto-optical phenomena that are closely connected with one another and in final analysis with the main magneto-optics phenomenon—the splitting of the energy states—which becomes most directly manifest in the splitting of spectral lines—the Zeeman effect.

Magneto-optical phenomena are observed as a rule in two experimental schemes: when the vector of the light wave \mathbf{K} is parallel to the magnetic field \mathbf{H} (the Faraday scheme) and when $\mathbf{K} \perp \mathbf{H}$ (the Voigt scheme).

In the former case (longitudinal observation), there can be observed either a difference between the refrac-

tive indices n_+ and n_- of two circularly-polarized components, a difference manifest in the rotation of the plane of polarization of linearly-polarized light (magneto-optic rotation (MOR)), or the Faraday effect, or else a difference between the absorption coefficients k_+ and k_- for these components (magnetic circular dichroism (MCD)). The latter can be determined either directly (upon inversion of the circular polarization of the light or of the magnetic-field direction), or by measuring the weak ellipticity that a linearly-polarized has acquired upon passing through a medium placed in a magnetic field.

In the second case (transverse observation), there may be observed birefringence connected with the difference between the refractive indices for the light that is linearly polarized parallel (π) and perpendicular (σ) to the magnetic field \mathbf{H} (the Voigt effect and the Cotton-Mouton effect that is quadratic in the field).

The Zeeman effect can be observed, as is well known, in both schemes (longitudinal and transverse effects).

In recent years, the investigation of MOR and of MCD has increased in popularity as a method for studying the structure of solids. This resumption of interest in long-known phenomena is connected with the development of solid-state spectroscopy, which makes possible a purposeful interpretation of observed phenomena and their regularities, as well as with the improvement of the experimental techniques, which makes it possible to perform precision experiments under extremal conditions of infralow temperatures and strong magnetic fields.

Unlike the Zeeman effect, an investigation of which calls for the presence of narrow spectral lines needed for the resolution of the components of the magnetic splitting in practical fields, MOR and MCD can be observed in the wide absorption bands characteristic of many systems. The study of MOR and MCD in the absorption-band region yields qualitative and quantitative information concerning both the ground and excited states of the system—the values of the magnetic splitting of the levels (the g -factors) and the symmetry of the states that take part in the optical transitions. In addition, it makes it possible to determine the local symmetry of the individual absorbing centers of the system, and by the same token to obtain a rigorous experimental criterion for the validity of any particular model of the center. Application of a magnetic field lifts all the residual degeneracies of the energy levels, thus increasing the information content of magneto-optical investigations compared with other methods of investigation in external fields.

The greatest progress in the investigation and interpretation of MOR and MCD has been reached in recent years for intrinsic and activator defects in cubic ionic crystals (color centers and activator centers) and complexes of transition metals.

The purpose of the present review is to give an idea, on the basis of the latest results, of the nature and methods of analyzing the dispersion of MOR and MCD, and of the possibilities uncovered by the investigation of these phenomena in the study of the structure of crystals. We shall not consider in this review the numerous investigations in the field of magneto-optics of semiconductors, which yield extensive information concerning the structure of the energy bands and which has been under intense investigation in the last decade. In this region, where, unlike in classical magneto-optics, one quantizes not the local levels of the individual centers but the states of the electrons in the bands, much progress has been reached, but the analysis is beyond the scope of the present review (see, for example, the review^[116]).

II. THEORY AND ANALYSIS OF THE DISPERSION CURVES OF MAGNETOOPTIC ROTATION AND MAGNETIC CIRCULAR DICHROISM

The phenomenological theory of magneto-optical phenomena, based on the notions of the difference between the macroscopic characteristics of the medium for two different circularly-polarized components, was developed already in the last century by Righi and Becquerel^[1], who showed that the explanation presented by Fresnel for the natural optical activity is applicable also to the Faraday effect. A review of work on circular anisotropy, performed prior to the early Thirties, is contained in the extensive article by Schutz^[2]. A quantum-mechanical theory of MOR and MCD was developed in the Thirties, particularly by Rosenfeld^[3], Kronig^[4], Kramers^[5], and Serber^[6]. With a few exceptions^[7], it describes satisfactorily the experiments in the field of transparency of various media (far from the absorption bands). The MOR dispersion in the region of absorption bands (the Macaluso-Corbino phenomenon) was qualitatively described, in particular, by Carol^[8]. Only relatively recently were theoretical expressions proposed for the dispersion MOR and MCD in the region of the absorption bands. A detailed bibliography of both theoretical and experimental papers related to this group of problems is contained in the extensive review of Buckingham and Stevens^[9] and in the bibliographical review of Palik and Henvis^[10].

1. Macroscopic Analysis

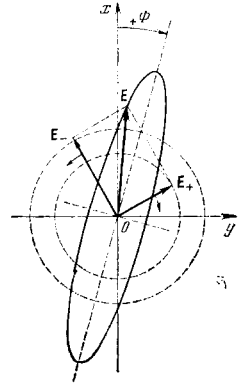
Let us consider a plane-polarized electromagnetic wave with angular frequency ω . We assume that the wave propagates in a positive direction of the z axis through an isotropic medium, for example a cubic crystal with complex refractive index $\hat{n} = n - ik$, which n and k are the usual (real) refractive index and absorption coefficient respectively. Such a wave can be represented in the form of a superposition of two circularly polarized waves of equal amplitude

$$\mathbf{E}(\omega) = \mathbf{E}_+(\omega) + \mathbf{E}_-(\omega), \quad (1)$$

where, in complex notation,

$$\mathbf{E}_\pm(\omega) = (i \pm ij) E_0(\omega) e^{i\omega t - \frac{\hat{n}_\pm z}{c}}. \quad (2)$$

FIG. 1. Passage of polarized light through an optically active medium. The linearly polarized light is transformed into elliptically-polarized light. The angle of rotation Φ of the major axis of the ellipse is determined by the phase difference of the components E_+ and E_- ; the ellipticity Θ is determined by the difference between the intensities of these components.



The plus and minus signs correspond here to right- and left-circular polarizations (Fig. 1). In the presence of a static magnetic field, the two circular oppositely-polarized components propagate with different velocities ($n_+ \neq n_-$), and furthermore they are absorbed at different rates ($k_+ \neq k_-$). As a result, an incident linearly-polarized light passing through a medium in the direction of the magnetic field is transformed into elliptically-polarized light (Fig. 1). In polarimetric experiments one measures either the angle of rotation Φ of the major axis of the ellipse relative to the plane of polarization of the incident light (the Faraday effect), or the degree of ellipticity Θ —the angle whose tangent is equal to the ratio of the minor and major axes of the ellipse (magnetic circular dichroism). In the notation employed, the angle of rotation Φ and the ellipticity Θ , measured in radians per unit length, are expressed in terms of the difference between the quantities n_\pm and k_\pm as follows:

$$\Phi = \frac{\omega}{2c} (n_+ - n_-), \quad (3a)$$

$$\Theta = \frac{\omega}{2c} (k_+ - k_-) = \frac{1}{4} (\alpha_+ - \alpha_-), \quad (3b)$$

where $\alpha = 2\omega k/c$.

The optical constants n and k can assume arbitrary values for each given frequency. However, if we regard $n(\omega)$ and $k(\omega)$ as functions of the frequency, then one of them, for example, $k(\omega)$ or $\alpha(\omega)$, being known in the frequency interval from 0 to ∞ , determines completely the other, $n(\omega)$. The character of this rather general relationship was first established by Kronig^[11] and by Kramers^[12]:

$$n(\omega) - 1 = \frac{2}{\pi} \int_0^\infty \omega' k(\omega') [\omega^2 - \omega'^2]^{-1} d\omega', \quad (4)$$

where the integral should be taken in the sense of the principal value^[13]. It is to be expected that analogous relations connect the frequency dependences of Φ and Θ , since they are in essence quantitative measures of the effects connected with the action of the crystal on two circularly-polarized components, for each of which there are dispersion relations of the Kramers-Kronig type (4).

To obtain the dispersion relations between Φ and Θ , we write down Maxwell's equations for a nonmagnetic medium:

$$[\nabla E] = -\frac{1}{c} \dot{H}, \tag{5}^*$$

$$[\nabla H] = \frac{1}{c} \dot{D}. \tag{6}$$

Eliminating H' from these equations, we obtain one equation relating the electric field intensity vector E with the electromagnetic induction vector D :

$$\nabla(\nabla \cdot E) - \nabla^2 E = -\frac{1}{c} \frac{\partial^2 D}{\partial t^2}. \tag{7}$$

The solution of (7) is sought in the form of a plane monochromatic wave (1) and (2). The response of the system to the electric field E of the light wave is characterized by the electromagnetic induction vector $D = E + 4\pi P$ (P —polarization vector of the medium), which is connected with E via the complex dielectric tensor $\epsilon_{ij}(\omega)$:

$$D_i(\omega) = \sum_j \epsilon_{ij}(\omega) E_j(\omega). \tag{8}$$

In the case of isotropic media, the tensor $\epsilon_{ij}(\omega)$ reduces to a single constant $\epsilon(\omega)$. An external static magnetic field lowers the symmetry of the system, and we return to the need for characterizing the response of the medium by means of the tensor $\bar{\epsilon}(\omega)$. It can be shown from symmetry considerations that in cubic crystals, independently of the orientation of the external static magnetic field (if we confine ourselves to effects of first order in the field), the tensor $\bar{\epsilon}(\omega)$ is given by^[14,15]

$$\bar{\epsilon}(\omega) = \begin{pmatrix} \epsilon_{xx} & \epsilon_{xy} & 0 \\ -\epsilon_{xy} & \epsilon_{yy} & 0 \\ 0 & 0 & \epsilon_{zz} \end{pmatrix}. \tag{9}$$

Equations (7) and (8) should be solved simultaneously with account taken of (1), (2), and (9). When nonmagnetic media that permit transmission investigations are considered, it is advantageous to simplify the problem by noting^[15] that in this case the refractive indices for the two circularly-polarized components n_{\pm} are close to each other: $n_{+} \approx n_{-} \approx n_0$, where n_0 is the refractive index of the medium in the absence of a magnetic field, and furthermore $n_{+}^2 - n_{-}^2 \gg k_{+}^2 - k_{-}^2$; then

$$n_{+}^2 - n_{-}^2 = 2\epsilon_{xy}^{(2)}, \tag{10}$$

$$n_0(k_{+} - k_{-}) = -\epsilon_{xy}^{(1)}, \tag{11}$$

where $\epsilon_{xy}^{(1)}$ and $\epsilon_{xy}^{(2)}$ are the real and imaginary parts of the components of the tensor ϵ_{xy} ($\epsilon_{xy} = \epsilon_{xy}^{(1)} + i\epsilon_{xy}^{(2)}$). In this approximation, the Faraday rotation angle Φ and the ellipticity Θ are written in the form

$$\Phi = \frac{\omega}{2cn_0} \epsilon_{xy}^{(2)}, \quad \Theta = -\frac{\omega}{2cn_0} \epsilon_{xy}^{(1)}. \tag{12}$$

To establish the dispersion relations connecting Φ and Θ , we can now use the well known relations between the real and imaginary parts of the dielectric tensor^[16]. As a result we obtain

$$\Phi(\omega) = -\frac{2}{\pi} \int_0^{\infty} \omega'^2 \Theta(\omega') [(\omega^2 - \omega'^2)\omega']^{-1} d\omega', \tag{13}$$

$$\Theta(\omega) = -\frac{2}{\pi} \int_0^{\infty} \omega \Phi(\omega') [|\omega^2 - \omega'^2|^{-1}] d\omega'. \tag{14}$$

A relation of the type (14) was used to find the character of the dispersion of magnetic circular dichroism by

measuring the dispersion of the Faraday rotation^[15].

The satisfactory agreement between the calculation results and direct measurements of MCD offer evidence of the advisability of using the dispersion relations (13) and (14) for the analysis of the dispersion of MOR and MCD in nonmagnetic media which lend themselves to transmission investigations.

2. Semiquantitative Analysis

The macroscopic analysis presented in Sec. 1 is suitable for regions far from the absorption bands ($n^2 \gg k^2$) and is based on the assumption that n and k differ for the two circularly-polarized components. The reasons for this difference, however, were not considered. Further development of the theory, particularly its extension to the region of the absorption bands, should be based on the primary phenomenon, namely the splitting of the energy levels in the magnetic field (the Zeeman effect). It is easy to verify that the character of the MOR and MCD dispersion curves in the region of the absorption bands can be established if one knows the character of this splitting and the relative intensities of the optical transitions in the left (σ_{-}) and right (σ_{+}) circular polarizations. In order to carry the formal analysis through to conclusion, let us consider the simplest case—a system with an odd number of electrons, in which the ground and nearest excited states form Kramers doublets, between which an electric dipole transition is allowed (Fig. 2, I). In this section, in the analysis of the dispersion of MOR and MCD, we shall assume that the contour of the corresponding absorption band is close to Gaussian in form

$$\alpha(E) = \alpha^{(0)} e^{[-(E-W)^2/\delta^2]}, \tag{15}$$

where E is the energy, $\alpha^{(0)}$ is the maximum value of the absorption coefficient ($\alpha^{(0)} = 2Wk^{(0)}/c\hbar$) at $E = W$, and δ is the width of the contour. When an external static magnetic field is applied, the Kramers doublets split. In accordance with the selection rules two optical transitions are realized in the system, one in

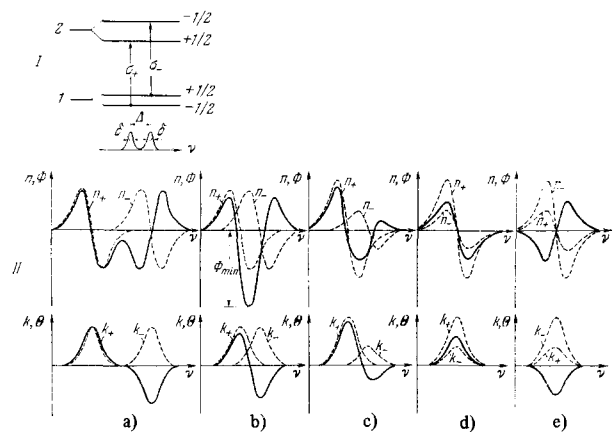


FIG. 2. Dispersion of MOR and MCD in systems described by the level scheme I. In Figs. II, the dashed curves represent the dispersion of n and k for individual components, while the solid curves represent the summary dispersion of Φ and Θ . a) $\Delta > \delta$, $n_{+} = n_{-}$, $k_{+} = k_{-}$; b) $\Delta \approx \delta$, $n_{+} = n_{-}$, $k_{+} = k_{-}$; c) $\Delta \approx \delta$, $n_{+} \neq n_{-}$, $k_{+} \neq k_{-}$; d) $\Delta < \delta$, $n_{+} > n_{-}$, $k_{+} > k_{-}$; e) $\Delta < \delta$, $n_{+} < n_{-}$, $k_{+} < k_{-}$.

* $[\nabla E] \equiv \nabla \times E$.

the polarization σ_+ , and the other in the polarization σ_- (π transitions in the system $\mathbf{K} \parallel \mathbf{H}$ can be disregarded). Thus, the contour of the absorption band in the magnetic field can be represented in the general case in the form of a sum of two contours of the type (15), which generally speaking are shifted in frequency ($W_+ \neq W_-$) and differ in intensity ($\alpha_+^{(0)} \neq \alpha_-^{(0)}$)*.

The last circumstance may be due either to a redistribution of the populations of the magnetic sublevels of the ground level under the conditions of thermal equilibrium or to the difference between the amplitudes of the optical σ_+ and σ_- transitions in the magnetic field. In real systems, these factors act, generally speaking, simultaneously and the main problem in the interpretation of MOR and MCD is to separate from the summary dispersion curves the individual contributions due to the different factors. Let us examine the character of the dispersion of the difference effects (3a) and (3d) in various particular cases. If the frequency shift of the σ_+ and σ_- components, $\Delta = W_+ - W_-$, greatly exceeds the width δ of the absorption band $\Delta \gg \delta$, then the MOR and MCD dispersion curves consist essentially of two individual curves $\Phi_+(E)$, $\Phi_-(E)$ and $\alpha_+(E)$, $\alpha_-(E)$. These curves overlap slightly (Fig. 2, II a), where it is assumed for simplicity that $\alpha_+^{(0)} = \alpha_-^{(0)}$. In order to transform the MCD contour into the MOR contour, we can use the dispersion relation (13) in the form

$$\Phi(E) = \frac{E^2}{2\pi} \int_0^\infty \alpha(E') |E'(E^2 - E'^2)|^{-1} dE'. \quad (16)$$

For the contours of type (15), the improper integral (16) can be calculated under the condition that $\delta \ll W$ ^[17,18], as is the case with all the optical phenomena of interest to us, and as a result we get

$$\Phi(E) = -\frac{\alpha^{(0)}}{2\sqrt{\pi}} \left\{ \frac{\delta}{W} + F\left(\frac{E-W}{\delta}\right) - \frac{\delta}{2(E+W)} \right\}, \quad (17)$$

where

$$F(x) = e^{-x^2} \int_0^x e^{y^2} dy, \quad x = \frac{E-W}{\delta}. \quad (18)$$

A plot of the function $F(x)$ is shown in Fig. 3^[19,20]. In the regions where $F(x)$ reaches a maximum, terms of the order δ/W can be neglected; then

$$\Phi(E) = -\frac{\alpha^{(0)}}{2\sqrt{\pi}} F\left(\frac{E-W}{\delta}\right). \quad (19)$$

In regions far from the center of the band, $E - W \gg \delta$, we have asymptotically

$$\Phi(E) = \frac{2\alpha^{(0)}}{\sqrt{\pi}} \frac{\delta}{W} \frac{E^2}{E^2 - W^2}. \quad (20)$$

The case considered above is encountered in crystals relatively rarely, principally for transitions within screened shells of rare-earth ions and iron-group transition-metal ions. The corresponding information can be obtained here also without making use of MOR or MCD, for example with the aid of the Zeeman-spectroscopy method. In this connection, the case of greatest interest is that of broad absorption bands, when the frequency shift of the components σ_+ and σ_-

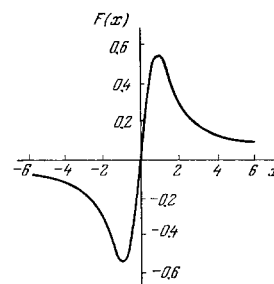


FIG. 3. Plot of the function

$$F(x) = e^{-x^2} \int_0^x e^{y^2} dy.$$

is $\Delta \ll \delta$. In this case an investigation of MOR and MCD is in essence the only source of information concerning the structure of the energy space and their splittings in the magnetic field. Characteristic MOR and MCD dispersion curves that can be observed in this case are shown in Figs. 2, II, b-e. In Fig. 2, II, b is shown a case when $\Delta \approx \delta$ and the intensities of the components k_+ and k_- are identical. In this case the MOR dispersion curve has a characteristic U-shape form and the MCD curve has a characteristic S-shape form. Fig. 2, II, c shows the form of the MOR and MCD dispersion curves in the case when $\Delta \approx \delta$, but the components have different intensities. Finally, Fig. 2, II, d-e show MOR and MCD dispersion curves for the limiting case when the shift of the bands is small ($\Delta \ll \delta$), but $k_+ > k_-$ or $k_- > k_+$. The extremal points of these curves can be used to estimate the parameters of the quantum-mechanical system.

On the basis of expression (19), it is easy to find a relation between the maximal (negative) value of the angle of rotation of the plane of polarization (Φ_{\min}) for the MOR dispersion curves of the type shown in Fig. 2, II, b with the value of the frequency shift of the σ_+ and σ_-

$$\Phi_{\min} = \left(\frac{\ln 2}{\pi}\right)^{1/2} \frac{\alpha^{(0)}}{\delta^{1/2}} \Delta. \quad (21)$$

This can be done also by relating the quantity Δ to the extremal points of MCD dispersion curve.

For the dispersion curves of the type 2, II, d-e, we obtain directly from (3b)

$$\Phi_{\text{extr}} = \frac{1}{4} |\alpha_+^{(0)} - \alpha_-^{(0)}|. \quad (22)$$

Starting from relation (19), we obtain also^[21]

$$\Phi_{\text{extr}} = \frac{1}{2\sqrt{\pi}} F_{\text{extr}} |\alpha_+^{(0)} - \alpha_-^{(0)}|. \quad (23)$$

In accordance with the foregoing, the difference $\alpha_+^{(0)} - \alpha_-^{(0)}$ can be due to the difference between the amplitudes of the optical σ_+ and σ_- transitions. Then $\alpha_+^{(0)} - \alpha_-^{(0)} \sim |\langle \dots | \hat{P}_+ | \dots \rangle|^2 - |\langle \dots | \hat{P}_- | \dots \rangle|^2$, where $\hat{P}_\pm = \hat{P}_x \pm i\hat{P}_y$, and relations (22) and (23) make it possible to estimate the parameters of the mutual influence of the states in the magnetic field ("mixing" of the states), which lead to a difference between the amplitudes of the optical σ_+ and σ_- transitions. On the other hand, if the g-factor of the ground state is not small, then the difference $\alpha_+^{(0)} - \alpha_-^{(0)}$ will be determined mainly by the difference of the populations of the magnetic sublevels of this state. Then $\alpha_+^{(0)}$

*We disregard here the changes in the contour shape when a magnetic field is applied (see below).

$-\alpha^{(0)} \sim \alpha^{(0)} \tanh(g_1 \beta H / 2kT)$. The Faraday rotation has in this case a temperature dependence characteristic of the paramagnetic susceptibility of the substance. In order to emphasize this fact, this case of Faraday rotation is sometimes called "paramagnetic." It is significant mainly at low temperatures. We note that in this case it is possible to determine the g-factor of the ground state from the temperature dependence of the MOR or MCD. The temperature-independent Faraday rotation due to the very fact of the splitting of the states in the magnetic field (Fig. 2, II, b) is sometimes called "diamagnetic" [9]. We shall henceforth use the terms "diamagnetic" and "paramagnetic" rotation only as convenient abbreviations.

The foregoing analysis of the dispersion of MOR and MCD was based essentially on a definite shape of the absorption band (in this section we considered an isolated band of Gaussian shape), and was carried out in the approximation of the so-called "rigid shift"—all the changes of the shape of the band in the presence of an external magnetic field were limited to a shift of the band as a whole (without a change in its shape), which is valid only for electron-vibrational bands due to the interaction of the electron transition with fully-symmetrical oscillations (in the absence of the Jahn-Teller effect, etc.). In [22-24] there was developed a method of analyzing magneto-optical experiments as applied to F-centers in alkali-halide crystals, making it possible to lift these limitations and to take into account the changes occurring in the contours of the absorption bands when an external magnetic field is applied. It is based on the use of the method of moments developed by Lax [25] as applied to the optical absorption of crystals. In Sec. 2 of Ch. III, this method will be considered in greater detail using concrete examples of color centers and impurity centers in crystals.

3. Microscopic Analysis

The most consistent analysis of the dispersion of MOR and MCD in the region of absorption bands can be made within the framework of the microscopic approach, by calculating Φ and Θ "from first principles," which reduces to quantum-mechanical calculations of the polarizabilities (susceptibilities) of the individual optically active centers in the presence of an external static magnetic field. Such a program was realized in part in [9, 26], where theoretical expressions were proposed for the dispersion of MOR and MCD in the region of the absorption bands, making it possible to cover a large group of magneto-optical experiments in $\mathbf{K} \parallel \mathbf{H}$ configurations. Following Buckingham and Stevens, we supplement Maxwell's equations (5) by the material equation relating the vectors \mathbf{E} and \mathbf{D} , in the form

$$\mathbf{D} = \mathbf{E} + 4\pi \sum_a N_a \mathbf{m}^a, \quad (24)$$

where \mathbf{m} is the electric moment induced by the electromagnetic field, and N_a is the number of optically active centers in the state a . For media having no natural optical activity

$$m_\nu = \sum_\mu \alpha_{\nu\mu} E_\mu, \quad \nu, \mu = x, y, z, \quad (25)$$

where $\alpha_{\nu\mu}$ is the electric polarizability tensor and is

a function of the static magnetic field H . Equations (6), (24), and (25) should be solved simultaneously with (1) and (2) taken into account, and yield as a result

$$\varphi = -\frac{i\pi\omega(n^2+2)^2}{9nc} \sum_a N_a (\alpha_{xy}^a - \alpha_{yx}^a), \quad (26)$$

where φ is the complex angle of rotation:

$$\varphi = \Phi - i\Theta. \quad (27)$$

We took into account here the difference between the external electric field and the field acting on the individual center in the condensed medium. Assuming a Lorentzian effective field, this leads to the appearance of a factor $(n^2+2)^2/9n$, where n is the average value of the refractive index. The electric polarizability tensor $\alpha_{\nu\mu}$ can be calculated quantum-mechanically [26, 27], and as a result, for a complex angle of rotation in the region of a group of transitions $a \rightarrow b$, we obtain in the considered approximation

$$\varphi = -\frac{4\pi(n^2+2)^2}{9\hbar nc} \sum_a N_a \hat{X}(\omega, \omega_{ba}) \omega^2 Q_\alpha(a \rightarrow b), \quad (28)$$

where $\hat{X}(\omega, \omega_{ba})$ is a complex function describing the form of the dispersion and absorption in the vicinity of the individual resonance ω_{ba} ,

$$X(\omega, \omega_{ba}) = g(\omega, \omega_{ba}) - if(\omega, \omega_{ba}), \quad (29)$$

and $Q_\alpha(a \rightarrow b)$ is the imaginary part of the product of the matrix elements of the dipole moment $\mathbf{m} = \sum_i \mathbf{e} r_i$

of the subsystem (of the separate optically-active center) over the states a and b :

$$Q_\alpha(a \rightarrow b) = \text{Im} \{ \langle a | \hat{m}_\alpha | b \rangle \langle b | \hat{m}_\alpha | a \rangle \}. \quad (30)$$

Introducing the oscillator strengths for two circularly-polarized components, proportional to the individual populations of the states a ,

$$f_{ba}^\pm = \frac{2m\omega_{ba}}{\hbar e^2} |\langle a | \hat{m}_\pm | b \rangle|^2 N_a, \quad (31)$$

where $\hat{m}_\pm = \hat{m}_x \pm i\hat{m}_y$, we can represent the expression for the complex rotation angle in the form

$$\varphi = -\frac{\pi e^2 (n^2+2)^2}{2mc \cdot 9n} \sum_{b,a} \hat{X}(\omega, \omega_{ba}) \frac{\omega^2}{\omega_{ba}^2} (f_{ba}^- - f_{ba}^+). \quad (32)$$

We see therefore that the Faraday rotation (the real part of φ) is proportional to the summary circular dichroism for all the transitions, with allowance for the corresponding dispersion factors [26]. The factors N_a , \hat{X} , and Q_α in (28) are functions of the static magnetic field H namely N_a via the Boltzmann factor, which determines the relative populations of the state a , X via ω_{ba} , and Q_α via the wave functions of the states a and b , perturbed by the field H . The corresponding quantities are expanded in powers of H and only the first-order quantities are retained as a rule. The concrete forms of the expressions depends on the form of the function \hat{X} and on the ratio of the quantities ω , ω_{ba} , Γ_{ba} , and kT and on the Zeeman splittings $\omega_{ba}^{(1)} H$ ($\omega_{ba} = \omega_{ba}^{(0)} + \omega_{ba}^{(1)} H$). For the case of an isolated broad absorption band described by the function $\hat{X}(\omega, \omega_{ba})$, and at not too low temperatures ($\hbar\omega_{ba}^{(1)} H \ll kT$), we obtain expressions of the type

$$\Phi(a \rightarrow b) = -\frac{4\pi(n^2+2)^2}{9\hbar nc} N_a^{(0)} \left[\omega^2 g'(\omega, \omega_{ba}) A + \omega^2 f(\omega, \omega_{ba}) \left(B + \frac{C}{kT} \right) \right] H.$$

$$\Theta(a \rightarrow b) = -\frac{4\pi(n^2 - 2)^2}{9\hbar nc} N_a^{(0)} \left[\omega^2 f'(\omega, \omega_{ba}) A + \omega^2 g(\omega, \omega_{ba}) \left(B + \frac{C}{kT} \right) \right] H, \quad (33)$$

where $g'(\omega, \omega_{ba})$ and $f'(\omega, \omega_{ba})$ are certain functions of the frequency and depend on the functions g and f , respectively, while A , B , and C are constants that do not depend on ω but depend on the parameters of the quantum-mechanical system.

On the basis of the statements made in Sec. 2, the temperature-independent A -term, due to the very fact of the Zeeman splitting of the energy levels a and b in the magnetic field, can be classified as diamagnetic; the temperature-dependent C -term, due to the difference between the populations of the magnetic sublevels of the ground state a can be classified as paramagnetic; the B -term is due to perturbations of the wave functions of the states a and b as a result of "mixing in" of wave functions of neighboring levels. The maximal values of the contributions of the A , B , and C terms to the magneto-optical rotation and to the circular dichroism for the bands of the form $\hat{X} = (\omega_{ab}^2 - \omega^2 + i\omega\Gamma_{ba})^{-1}$, corresponding to a damped oscillator, are listed in Table I. Expressions similar to (33) were first derived by Serber^[6] for the case $\omega_{ba} - \omega \gg \Gamma_{ba}$ (far from the absorption bands) as a generalization of the initial Kramers formula^[5]. They are valid only for bands due to the electric-dipole transitions. A generalization of the initial Kramers formula with allowance for transitions of another type—electric-quadrupole and magnetic-dipole—was given by Shen^[26] for bands having a Lorentz shape. In this case the expressions (31) for the oscillator strengths contain, besides the electric-dipole term, also the electric-quadrupole and magnetic-dipole terms.

III. EXPERIMENTAL METHODS AND ANALYSIS OF CONCRETE SYSTEMS

As was already noted, the obvious application of the MOR and MCD methods for the study of crystals is for isotropic systems having broad absorption bands, for which the Zeeman method is therefore useless. Indeed, most investigations were performed with such systems, particularly with cubic crystals of alkali-halide and alkali-earth-halide salts, containing color centers and activator centers, among which a prominent position is assumed by centers produced by rare-earth activators. Many investigations were performed with complexes of transition metals having incomplete d shells. We present below the main results of these investigations,

Table I. Maximum values of the contributions of terms A , B , and C to the MOR and MCD

	$\Phi(a \rightarrow b) \frac{\hbar c}{4\pi N_a^{(0)}}$	$\Theta(a \rightarrow b) \frac{\hbar c}{4\pi N_a^{(0)}}$
A	$\frac{9\omega_{ba}^{(0)} A}{4\Gamma_{ba}^2 \hbar}$	$\frac{3\sqrt{3}\omega_{ba}^{(0)} A}{2\Gamma_{ba}^2 \hbar}$
B	$\frac{\omega_{ba}^{(0)} B}{\Gamma_{ba}}$	$\frac{\omega_{ba}^{(0)} B}{\Gamma_{ba}}$
C	$\frac{\omega_{ba}^{(0)} C}{\Gamma_{ba} kT}$	$\frac{\omega_{ba}^{(0)} C}{\Gamma_{ba} kT}$

prefacing them with a brief description of the employed experimental procedures.

1. Experimental Methods for the Investigation of MOR and MCD in Crystals

The measurement of MOR and MCD reduces to a determination of the angle of rotation of the polarization plane of plane-polarized light passing through the sample, when the latter is placed in a longitudinal magnetic field (MOR), or the difference between the absorption coefficients of the sample for two opposite directions of circular polarization of the transmitted light (MCD). The systems used for the observation of MOR and MCD do not differ in principle from those employed in the study of natural optical activity or natural circular dichroism^[17,18]; the main difference lies in the presence of a magnetic field, which is produced in most modern installations by means of superconducting solenoids. Fields of 5–50 kOe are customarily used. Inasmuch as the main information is extracted from dispersion curves, the variable element of the apparatus is a monochromator that scans the wavelength of the transmitted light. For the investigation of paramagnetic effects, deep cooling of the samples, frequently to subhelium temperatures, is employed.

In measurement of MOR one customarily employs phase methods in which the sample is placed between immobile or rotating polarizers, and the phase difference of the modulation of the measuring and reference light beams following application of a magnetic field is determined (Fig. 4a). Schemes are also possible based on a comparison of the intensities of light beams passing through a sample placed between polarizers, using two directions of the magnetic field (Fig. 4b). To obtain maximum sensitivity it is advantageous in this case to orient the polarizers in such a way that their axes make an angle of 45° ^[29].

A typical experimental setup, based on the phase-measuring principle, is shown in Fig. 5^[18]. The accuracy with which the angle of rotation of the plane of polarization is determined in good modern spectrum-polarimetric installations reaches 0.001° . To eliminate the rotation due to the main material of the investigated system (the matrix crystal), many installations are provided with the devices employed in many investiga-

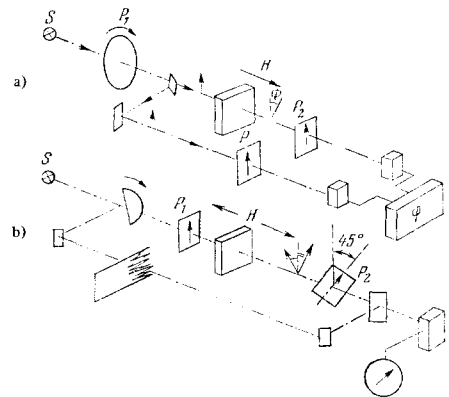


FIG. 4. Experimental setups for the measurement of MOR. a) Phase-symmetrical system; b) system with inversion of the magnetic field.

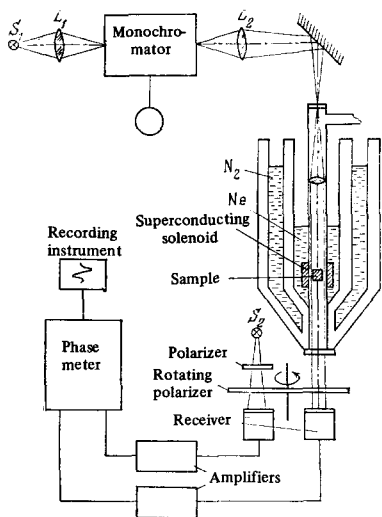


FIG. 5. Diagram of phase-meter setup for the measurement of MOR (from [18]).

tions of solutions, wherein this rotation is compensated by transmitting the light additionally through a similar crystal that does not contain the investigated centers and is placed in a magnetic field of opposite direction.

The MCD can be measured, for example, by using a very simple system with reversal of the magnetic field (Fig. 6a)^[30]. It is more convenient, however, to place a rotating achromatic $\lambda/4$ plate between the sample and the polarizer (Fig. 6b). In this case the state of the polarization of the light incident on the sample varies periodically, changing from circular polarization in one direction to the opposite polarization via a linear polarization state. In the presence of MCD, the receiver registers a signal modulated at double the frequency of rotation of the $\lambda/4$ plate. The rotating $\lambda/4$ plate can be replaced by an adjustable Pockels cell (see^[31]).

Sufficiently detailed descriptions of installations for the measurement of MOR and MCD can be found in many original papers^[15, 18, 23, 24, 31-33]. Many papers are devoted especially to the description of spectropolarimeters^[36].

2. Color Centers and Impurity Centers in Crystals

The advisability of using magneto-optical rotation for the study of color centers and impurity centers in crystals was pointed out by Dexter as early as in 1958^[37]. The experimental investigations were started five years later, and have grown considerably in scale

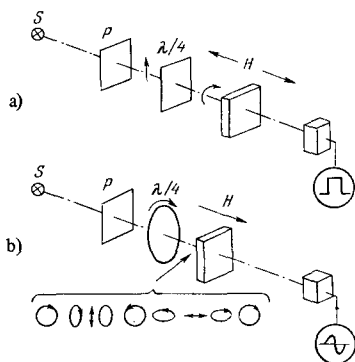


FIG. 6. Experimental setups for the measurement of MCD. a) System with inversion of the magnetic field; b) system with modulation of ellipticity.

by now. The main purposes of the heretofore performed magneto-optical investigations are the following: 1) investigation of the fine structure of the electronic levels that determine the broad absorption bands of the intrinsic and impurity defects; 2) investigation of the electron-vibrational interactions in crystal; 3) determination of criteria for the verification of the adequacy of models proposed for the centers, and 4) identification of absorption bands of color centers and impurity centers in less thoroughly investigated materials (rare-earth fluorides, oxides, etc.).

The absorption bands due to elementary intrinsic crystal-lattice defects in alkali-halide crystals—F centers—have an appreciable width ($\sim 2000 \text{ cm}^{-1}$), and are determined by optical transitions between the electronic states of type 2S and 2P , which interact strongly with the lattice vibrations.

The presence of a fine structure of the excited state of F centers (spin-orbit splitting of the 2P terms) was first established by MCD investigation in colored KBr crystals^[30]. The spectral behavior of the absorption-

coefficient difference $k_{1/2}^{\sigma_+, \nu} - k_{-1/2}^{\sigma_+, \nu}$ for transitions from two magnetic sublevels of the ground state $^2S(|+\frac{1}{2}\rangle$ and $|-\frac{1}{2}\rangle$) was measured at a temperature 1.85°K in circularly-polarized light with two mutually-opposite directions of the magnetic field (Fig. 7). Knowing the spectral dependence of $k^\nu = (\frac{1}{2})(k_{1/2}^{\sigma_+, \nu} + k_{-1/2}^{\sigma_+, \nu})$ in the absence of the field, it is possible to determine separately the absorption coefficients $k_{1/2}^{\sigma_+, \nu}$ and $k_{-1/2}^{\sigma_+, \nu}$. They represent two similar curves spaced 130 cm^{-1} apart (Fig. 7).

These results can be interpreted with the aid of the system of energy levels of the F centers in the "alkali-atom model" (Fig. 8). The fine-structure parameter Δ —the magnitude of the spin-orbit splitting of the state 2P —is negative, i.e., the level $^2P_{1/2}$ lies above the level $^2P_{3/2}$. If we take into consideration the relative intensities of the transitions in the polarization σ_+ , then we find that $2\Delta/3 = 130 \text{ cm}^{-1}$, i.e., $\Delta \approx 200 \text{ cm}^{-1}$. Using an intense source of excitation by means of circularly-polarized light, it was possible to effect an appreciable inversion of the populations of the states $|+\frac{1}{2}\rangle$ and $|-\frac{1}{2}\rangle$. An investigation of the fine structure by measuring the MOR dispersion was first performed for the absorption F band in KCl^[38]. Figure 9 shows by way of a characteristic example (from the data of^[18]) the spectral dependence of the MOR of additively-colored KCl crystals at temperatures 4.2 and 65°K . The MOR dispersion curve coincides in its

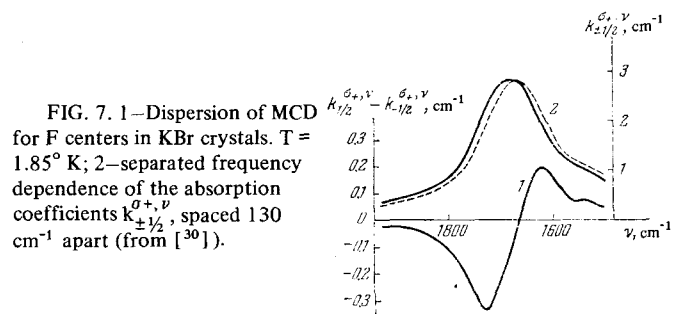


FIG. 7. 1—Dispersion of MCD for F centers in KBr crystals. $T = 1.85^\circ\text{K}$; 2—separated frequency dependence of the absorption coefficients $k_{\pm 1/2}^{\sigma_+, \nu}$, spaced 130 cm^{-1} apart (from [30]).

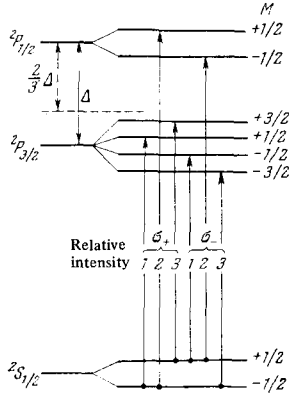


FIG. 8. Energy level scheme of F center ("alkali atom model").

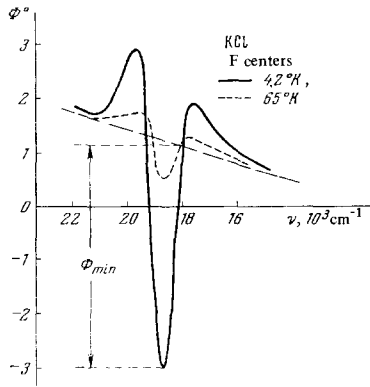


FIG. 9. Dispersion of MOR in the region of the absorption F band of additively colored KCl crystals at 4.2 and 65° K (from [18]).

character with that shown in Fig. 2, II, b. If it is assumed that the shape of the F band is close to Gaussian^[15], then we can use formula (21) for the maximum (negative angle of rotation of the polarization plane Φ_{\min}). The effective energy shift ΔE can be estimated with the aid of the level scheme (Fig. 8), and as a result we get^[18]

$$\Delta E = \frac{(g_3 - 5g_2\nu)\beta H}{3} - \frac{2}{3} \operatorname{th} \left(\frac{g_1 \beta H}{2kT} \right) \Delta, \quad (34)$$

where g_2 and g_3 are the spectroscopic-splitting factors of the states ${}^2P_{3/2}$ and ${}^2P_{1/2}$ respectively. Combining expressions (21) and (34), we can obtain a formula for Φ_{\min} at not too low temperatures

$$\Phi_{\min} = - \left(\frac{\ln 2}{\pi} \right)^{1/2} \frac{\alpha^{(0)} \beta H}{\delta_{1/2}} \left(\frac{g_3 - 5g_2\nu}{3} - \frac{g_1 \Delta}{3kT} \right), \quad (35)$$

where $\delta_{1/2}$ is the half-width of the absorption band. The first term in (35) describes diamagnetic Faraday rotation Φ_{dia} , and the second paramagnetic rotation Φ_{para} , which depends on the spin-orbit splitting of the state 2P . Thus, the parameter Δ can be determined from the temperature dependence of the ratio $\Phi_{\text{para}}/\Phi_{\text{dia}} = -(\frac{9}{11})\Delta/3kT$.

In the "alkali-atom" model, no account is taken at all of the influence of the lattice vibrations of the degenerate excited state of the F center. Since the width of the band exceeds by one order of magnitude the measured value of the spin-orbit splitting Δ , the interaction between the F centers and non-cubic lattice vibrations can be expected to lift the degeneracy of the orbital P state and makes it impossible to describe it in terms of the orbital angular momentum (the Jahn-

Teller effect). In the "alkali-atom model," in addition, it is impossible to predict the change of the shape of the F band when a magnetic field is applied, since this shape is determined by the influence of the lattice vibrations (to interpret the experimental data it is necessary in this case to use the "rigid shift" approximation (Ch. III, Sec. 2)). A much more rigorous analysis of the magneto-optical experiments on F centers was presented by Henry et al.^[22], where the rather approximate energy level scheme of the F center in the "alkali-atom model" was not used, and it was proposed that: 1) the F center has cubic symmetry and 2) the F band is due to the transition from the symmetry state Γ_1 -orbital singlet-to the symmetry state Γ_4 -orbital triplet.

The analysis was carried out within the framework of the method of moments. The changes in the optical-absorption bands were described in terms of changes of the shape function of the absorption band $f(E)$, which is connected with the absorption coefficient $\alpha(E)$ by the relation

$$f(E) = \frac{C\alpha(E)}{E}, \quad (36)$$

where C is a constant characteristic of the system under consideration. The moments of the function $f(E)$ were determined in the following manner. The area or the zeroth moment is

$$A = \int f(E) dE. \quad (37)$$

The first moment or the center of gravity of the band is

$$\bar{E} = A^{-1} \int E f(E) dE. \quad (38)$$

The higher-order moments are

$$\langle E^n \rangle = A^{-1} \int (E - \bar{E})^n f(E) dE, \quad n \geq 2. \quad (39)$$

When a longitudinal magnetic field is applied, the contour of the absorption band, observed in right- or left-hand circular polarizations, changes in general in such a way that $f_{\pm}(E)$ is replaced by $f_{\pm}(E) + \Delta f_{\pm}(E)$. The changes of the moments are of the form

$$\langle \Delta E_{\pm}^n \rangle = A_{\pm}^{-1} \int (E - \bar{E}_{\pm})^n \Delta f_{\pm}(E) dE. \quad (40)$$

They can be calculated on the basis of MCD data, since $\Theta(E) \sim f_{+}(E)$. Indeed, according to (3b) we have $\Theta(E) \sim \Delta f_{+}(E) - \Delta f_{-}(E)$, but $\Delta f_{+}(E) = -\Delta f_{-}(E)$, so that $\Delta f_{+}(E) - \Delta f_{-}(E) = 2\Delta f_{+}(E)$. On the other hand, the changes of the moments can be related to the quantum characteristics of the system.

Under a number of simplifying assumptions (absence of anharmonicity, no mixing of the states, and a definite limitation on the electron-phonon interaction), the change of the first moment of the F band (the change of the center of gravity—the shift), observed in right- or left-hand circular polarizations, was calculated to be

$$\langle \Delta E_{\pm} \rangle = \pm g_{\text{orb}} (\beta H + \lambda \langle S_z \rangle), \quad (41)$$

where $g_{\text{orb}} = |\langle \mathbf{x} | \mathbf{L}_z | \mathbf{y} \rangle|$, λ is the spin-orbital coupling constant,

$$\langle S_z \rangle = -\frac{1}{2} \operatorname{th} \left(\frac{\beta H}{kT} \right) = -\frac{1}{2} \left(\frac{\beta H}{kT} \right). \quad (42)$$

With the aid of (41) it is possible to obtain a more rigorous expression for the effective energy shift $\Delta E = \Delta E_+ - \Delta E_-$ in formula (21):

$$\Delta E = 2\beta H g_{\text{orb}} + \frac{4}{3} \Delta \langle S_z \rangle, \quad (43)$$

where $\Delta = (\frac{3}{2})\lambda g_{\text{orb}}$ is the spin-orbit splitting of the 2P term. Then the ratio $\Phi_{\text{para}}/\Phi_{\text{dia}}$ assumes the form

$$\frac{\Phi_{\text{para}}}{\Phi_{\text{dia}}} = -\frac{9}{11} \frac{\Delta}{3g_{\text{orb}}kT}. \quad (44)$$

For purely atomic P states we have $g_{\text{orb}} = 1$, and we obtain the same result as in the "alkali atom model." In a cubic crystal field, g_{orb} may differ from unity.

Under the same assumptions it was shown, furthermore, that the area or the zeroth moment of the band is not changed by a field H, i.e.,

$$\langle \Delta E^0 \rangle = 0. \quad (45)$$

In the calculation of the changes of the higher moments of the band, the Zeeman splitting was not taken into account (in expression (41) it is necessary simply to omit the diamagnetic term). The result being

$$\langle \Delta E_{\pm} \rangle = \pm 2 \left(\frac{\Delta}{3} \right) \langle S_z \rangle, \quad (46)$$

$$\langle \Delta E_{\pm}^2 \rangle = \mp 2 \left(\frac{\Delta}{3} \right)^2 \langle S_z \rangle, \quad (47)$$

$$\langle \Delta E_{\pm}^3 \rangle = 3 \langle \Delta E_{\pm} \rangle \left[\langle E^2 \rangle_{\text{cub}} + \frac{1}{2} \left(\langle E^2 \rangle_{\text{noncub}} + \frac{2}{3} \left(\frac{\Delta}{3} \right)^2 \right) \right]. \quad (48)$$

Here $\langle E^2 \rangle_{\text{cub}}$ and $\langle E^2 \rangle_{\text{noncub}}$ are the contributions made to the second moment of the band by interactions with cubic and noncubic lattice vibrations:

$$\langle E^2 \rangle = \langle E^2 \rangle_{\text{cub}} + \langle E^2 \rangle_{\text{noncub}} + 2 \left(\frac{\Delta}{3} \right)^2. \quad (49)$$

In this approximation, the parameter Δ can be determined by measuring $\langle \Delta E_+ \rangle$ and using (46). The relation $x = \langle E^2 \rangle_{\text{noncub}}/\langle E^2 \rangle_{\text{cub}}$ can be obtained by measuring the quantities $\langle \Delta E_+ \rangle$, $\langle E^2 \rangle$, and $\langle \Delta E_+^3 \rangle$ and using (48) subject to the condition (49). The parameter x characterizes essentially the fraction of the Jahn-Teller distortions of the cubic center.

The complete system of equations of the method of moments, (45)–(49), was first used to interpret the MCD data obtained in the investigation of F centers in CsBr and CsCl crystals^[39,40], where the absorption F bands have a partly resolved structure. For CsBr, measurement of $\langle \Delta E_{\pm} \rangle$ yields $\Delta = 332 \pm 40 \text{ cm}^{-1}$ (measurement of $\langle \Delta E_{\pm}^2 \rangle$ yields the very close value $\Delta = 333 \pm 50 \text{ cm}^{-1}$). Measurements of the quantities $\langle E^2 \rangle$ (in the absence of a field), and $\langle \Delta E_{\pm}^3 \rangle$ leads to values $\langle E^2 \rangle_{\text{cub}} = (218 \pm 40 \text{ cm}^{-1})^2$ and $\langle E^2 \rangle_{\text{noncub}} = (289 \pm 50 \text{ cm}^{-1})^2$. The value of Δ obtained in this manner does not agree with the energy interval between the two partly resolved peaks in the spectrum of the F centers in CsBr (630 cm^{-1}). If these two peaks are connected with transitions to the states $^2P_{3/2}$ and $^2P_{1/2}$, then the discrepancy can be attributed to the fact that the noncubic types of oscillations "mix" the states $^2P_{3/2}$ and $^2P_{1/2}$, causing their mutual repulsion. An estimate of the magnitude of the splitting, with allowance for the repulsion, yields a value $\Delta \approx 600 \text{ cm}^{-1}$. A similar analysis was made also for F centers in CsCl and KCl^[23]. For the F centers in KCl, in

particular, it was found that $x = \langle E^2 \rangle_{\text{noncub}}/\langle E^2 \rangle_{\text{cub}} = 1.10 \pm 0.11$. The data obtained with the aid of the MCD investigation offer evidence that the fraction of the Jahn-Teller distortions of the cubic F center in the crystals under consideration is quite appreciable.

A summary of the data obtained by the investigation of MOR and MCD for F centers in alkali-halide crystals is given in Table II, which is taken from Margerie's paper at the Conference on Color Centers (Saclay, 1967)^[42].

A number of papers^[23,43-45] are devoted to the nature of the centers responsible for the so-called K-band, observed in the short-wave side of the F band in a number of alkali-halide crystals. A number of hypotheses have been advanced with respect to the nature of this band. An investigation of MCD^[23,43,45] and MOR^[44] in RbCl crystals and others has shown that the K band is due to the same F centers and is connected with transitions of these centers to higher excited states (transitions of the type $1s \rightarrow 3p, 4p, \dots$, etc.). Just as for the F band, the spin-orbit splitting is negative.

In the cited paper^[23], they investigated besides the ordinary F centers also the MCD of the so-called F_A centers produced in alkali-halide crystals in which an extraneous alkali metal is introduced as an impurity, and constituting F centers in a non-cubic crystalline field. The tetragonal distortion due to the presence of foreign ions near the F centers leads to a lifting of the three-fold orbital degeneracy of the excited states and to a splitting of the F band. The experimentally observed behavior of KCl-Na crystals in a magnetic field agrees fully with the behavior expected on the basis of a preliminary theoretical analysis^[22].

Table II. Spin-orbit splitting (Δ and g factors for F centers in alkali-halide crystals)

Crystal	Δ, cm^{-1}	g	Method
NaCl	-57 ± 9 -41 ± 8	2.6	MCD *) MOR
NaBr	-228 ± 50		MCD
KF	-40 ± 7		MCD *)
KCl	-61 ± 12 $-9, 2 \pm 19$	0.95 ± 0.1 1.3 ± 0.1 1.6	MCD *) MCD MOR
KBr	-186 ± 15 -188 ± 15 -155 ± 31	$1.4 \pm 0, 1$ 2.1	MCD *) MCD MOR
KJ	-320 ± 50 -242 ± 26	1.2	MCD *) MOR
RbCl	-140 ± 15 -204 ± 10		MCD *) MOR
RbBr	-205 ± 20 -261 ± 52		MCD *) MOR
CsCl	-300		MCD *)
CsBr	-330 -340 ± 68	2.8	MCD *) MOR
CsI	-300 ± 20		MCD *)

*The method of moments was used in the data reduction.

FA centers are related to Z centers, which were observed in alkali-halide crystals with alkali-earth ion impurities. The MCD of Z_1 centers produced in RbCl-Sr crystals by exposure to x-rays and subsequent irradiation at -30°C was investigated in^[46] at 1.9°K . Just as for F centers, the sign of Δ turned out to be negative, and the absolute magnitude of Δ amounted to approximately 120 cm^{-1} . Analyzing the results, the authors have reached the conclusion that the models of Seitz and Pick are in error, and that a model suitable for the description of Z_1 centers is that proposed by Hartel and Luty^[47] (electron localized in a cation-anion vacancy near the impurity ion).

A similar conclusion was reached by the authors of^[106], who analyzed in the "rigid shift" approximation the dispersion of MOR in the region of the Z_1 band in the crystal KCl-Oa, Sr at $T = 4.2^\circ\text{K}$.

Besides the simplest F centers, complicated aggregate centers, including several F centers, or centers representing associations of F centers with vacancies of one sign or another, can be produced in non-activated ionic crystals. Double F_2 centers (M centers) have a ground state of the type 1S_0 and cannot exhibit paramagnetic rotation. Triple R centers, modeled by an aggregate of three F centers forming a triangle in the (111) plane, were investigated in KCl crystals at 3.1°K by the MCD method^[48]. In full agreement with the hypothesis by Silsbee^[49], it was established that the ground state of the R center can be treated as an orbital doublet with 2E symmetry (in accordance with the C_{3h} symmetry group of the R center) with spin-orbit interaction reduced by the dynamic Jahn-Teller effect. The Jahn-Teller effect decreases in this case the orbital momentum of the system $b\Lambda$ (here Λ is the orbital momentum of the undeformed center and b is the Jahn-Teller reducing factor), and with it also the magnitude of the spin orbit interaction $\Lambda\lambda b$. The corresponding decreases of $b\Lambda$ and $\Lambda\lambda b$, however, are noticeably different, and this may be due to internal stresses (deformations) in the crystal, which greatly influence the magnitude of the MCD effect.

The influence of deformations on the magnitude of the MCD effect was demonstrated in^[50], where MCD was investigated under conditions of directional deformations both in the narrow phononless absorption line and in the region of the broad electron-vibrational structure of the R_2 band produced in KCl and KF crystals by an electronic transition in the R center from the ground state 2E into the excited state 2A_2 . An analysis of the experimental data was carried out with the aid of the method of moments under the assumption that the magnetic interactions in the R center, compared with the deformation interactions, can be regarded as a perturbation and the average magnitude of the internal stresses in the crystal can be approximately estimated. Investigations were made of the change of the zeroth and first moments for the phononless line in the presence of a magnetic field. The changes of the zeroth moment (the area under the phononless line) exhibit a dependence on the stresses in the sample. In the region of the electron-vibrational structure of the R_2 band, the changes of the zeroth moment A following application of a magnetic field, $dA(H)$, were calculated in accordance with (37) for

transitions including an even number of E phonons non-fully-symmetrical lattice vibrations of type E)

$$dA(H) = \frac{n_y - n_x}{n_y + n_x} \epsilon \sqrt{3}, \quad (50)$$

and an odd number of E phonons

$$dA(H) = -\frac{n_y - n_x}{n_y + n_x} \epsilon \sqrt{3}. \quad (51)$$

Here n_x and n_y are the populations of the sublevels of the ground state (the splitting has mainly a deformation character and is practically independent of the field H), and ϵ is a small parameter proportional to H , characterizing the degree of "mixing" of the wave functions of these sublevels in the magnetic field. (It is precisely this "mixing" of states which leads in this case to the observed MCD effect.) The difference between the signs in expressions (50) and (51) makes it possible to employ MCD data in the region of electron-vibrational structure to determine whether an even or an odd number of E phonons takes part in the formation of the given absorption peak, for in the latter case the MCD signal would have sign opposite to that of the MCD signal on a purely electronic phononless line, which coincides also with the MCD signal on transitions in which an even number of E phonons take part. In the given case of the R_2 band in KCl and KF, the MCD signal has no "negative" peaks, but certain peaks in the absorption correlate with the minima in the MCD signal.

A thorough investigation of R centers in the KCl crystal by means of MCD was undertaken in^[107]. The MCD was measured both in the region of the R_2 band and in the region of the R_1 band due to the electronic transition to the doubly-degenerate excited state ($E \rightarrow E$ transition). The dispersion curves were analyzed with the aid of the method of moments, applied to the case of a degenerate ground state (just as in^[50], only changes of the zeroth and first moments were investigated). With respect to the R_2 band, the data of these investigations are in good agreement. The results of investigations of MCD for the R_1 band confirm the conclusion that the excited state for the R_1 transition belongs to the E-type with weak Jahn-Teller distortion.

The MCD method was also used to investigate R' centers (four-electron system obtained by adding one more electron to the R center) in the LiF crystal^[108]. The MCD was measured on the 8328 \AA phononless R' line in order to determine the multiplicities of the states A and E that take part in the optical transition. The observed MCD is similar in shape to that shown in Fig. 2, II, b, i.e., it is proportional to the derivative of the line shape, with a proportionality coefficient $-\gamma$, where γ is the effective energy shift of the σ_+ and σ_- components of the type (43). The measured temperature dependence of the MCD presupposes that $\langle S_z \rangle \equiv 0$. This makes it possible to set the R' line in correspondence with the transition between the triplet states 3A and 3E . It was also established that the parameter of the spin-orbit coupling is positive in the case of the R' center (it is negative in the case of the F center).

Besides the intrinsic defects—electron and hole color centers—broad absorption bands may be produced in ionic crystals by defects connected with the presence

of foreign ions in the crystal lattice, and unlike the already mentioned FZ and Z centers, optical transitions between the levels of these ions are responsible for the absorption. An investigation of MOR and MCD of such ("activator") centers may yield information concerning their energy and geometrical structure.

As established by EPR investigations^[51], when KCl crystals activated with silver are exposed to x-rays ($T = 77^\circ\text{K}$), two types of defects are produced: V_K centers (Cl_2^-) and neutral silver atoms Ag^0 , which have as the ground state $^2S_{1/2}$ (configuration $4d^{10}5s$). The absorption band near 23600 cm^{-1} is due apparently to transitions of the $^2S \rightarrow ^2P$ type in Ag^0 atoms. The band overlapping with it, connected with a transition of the $^2\Sigma \rightarrow ^2\Sigma$ type in the V_K center, makes no contribution to the rotation. The MOR dispersion in the region of these bands was investigated in^[24] (Fig. 10). The asymmetry in MOR picture is due in part to the asymmetry of the unperturbed contour of the absorption band, and in part to changes in the higher moments of the shape function of the band when the field is applied.

The observed contour of the MOR curve was transformed with the aid of the dispersion relation (14) into a MCD contour, and then the first moment was calculated. The parameter $\lambda' = 2\Delta/3$ obtained in this manner, which determines the fine structure of the excited state 2P of the Ag^0 atom, amounts to 370 cm^{-1} in KCl, and is approximately half as large as the corresponding value for the free atom (613 cm^{-1}). This discrepancy can be ascribed to the influence of covalence effects^[24,52].

With the aid of the MCD method, investigations were made also of the A band of impurity absorption in KI-Tl, KBr-Pb, KBr-Tl, and KCl-Pb crystals^[31]. These bands are connected with spin-forbidden transitions $^1S_0 \rightarrow ^3P_1$ and $(6s)^2 \rightarrow (6s)(6p)$ in the Tl^+ and Pb^{2+} ions (the transitions are due to the admixture of singlet 1P states as a result of spin-orbit interaction). The g-factors of the excited state were determined with the aid of relation (43), where $\langle S_Z \rangle = 0$. The expected value of the g factor for the state 3P_1 in the free-ion approximation is 1.4. The reasons why the experimental values turned out to be much smaller (0.6–0.8) are not quite clear, but here, too, covalence effects can play an important role.

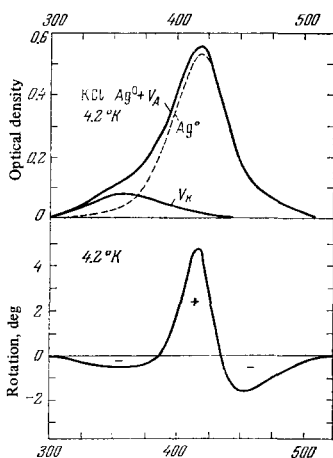


FIG. 10. MOR dispersion in the region of the atomic bands (Ag^0) in irradiated KCl-Ag crystals ($T = 4.2^\circ\text{K}$) (from^[24]).

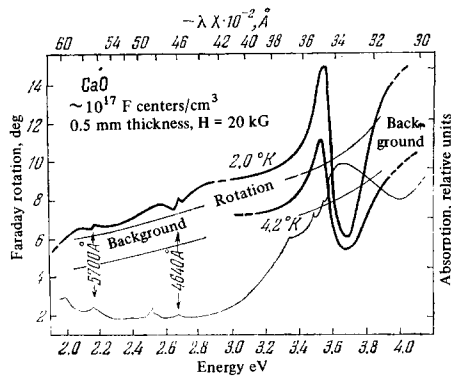
In^[109], the MCD method was used to investigate the A bands of impurity absorption in KCl-In, KBr-In, and KI-In, connected with the transition of the indium ions (In^+) to a triply-degenerate excited state $(5s)^2\ ^1S_0 \rightarrow (5s)(5p)^3P_1$. An analysis of the form of the MCD dispersion curves has confirmed the theoretical conclusion^[110] that a doublet structure of the A absorption bands is present in these crystals, due to the dynamic Jahn-Teller effect.

All the investigations referred to so far were carried out with "pure" and activated alkali-halide crystals. Of course, this group of objects does not limit the regions of applicability of the MOR and MCD methods. In^[53] it was indicated, on the basis of an EPR investigation that F centers exist in crystals of alkali-earth fluorides. The optical absorption spectra of additively colored samples of CaF_2 , SrF_2 , and BaF_2 are quite complicated, for in addition to the F bands these crystals reveal also many other bands of comparable intensity, due apparently to aggregates of F centers^[54]. The positions of the maxima of the absorption F bands in such a situation can be established by investigating the MOR (or MCD) dispersion^[55], since the aggregate states, unlike the F centers, are not paramagnetic. The positions of the maxima observed experimentally at 4.2°K ^[55] agree with the results of the calculation^[56,57] (see Table III).

Table III. Positions of the maxima of the F band and values of the spin-orbit interaction constants λ in alkali-earth fluorides (from^[55])

Crystal	Positions of maxima			λ, cm^{-1}
	Observations 4.2°K	Theory ⁵⁶	Theory ⁵⁷	
CaF_2	376	388	380	~ 44
SrF_2	435	426	—	— 66
BaF_2	611	475	670	— 50

The MOR dispersion in crystals of alkali-earth oxides (MgO and CaO) irradiated with neutrons was investigated in^[32a]. The absorption spectra of the irradiated crystals consist of broad intense bands in the ultraviolet region at narrow peaks and associated bands in the visible region. Ultraviolet bands can be ascribed to transitions in F centers^[58-60]. The MOR dispersion was investigated in greatest detail for CaO crystals (Fig. 11), in which these bands lie in a relatively longer wavelength region of the spectrum, thus eliminating a number of experimental difficulties (insufficient transmission, etc.). The characteristic peak of the MOR curve near 3.7 eV, ascribed to the F centers, is distorted on the short-wave side by the increasing background, by instrumental limitations, and by the influence of bands connected with other defects. To refine the character of the MOR dispersion in this region, the double resonance effect was investigated^[61]. Inversion of the spin system (up to 80%) was produced by application of microwave radiation and rapid adiabatic passage of the magnetic field through the resonant value ($g = 2.0001$). The change of the rotation angle $\Delta\Phi$ was equal in this case to double the paramagnetic Faraday effect Φ_{para} . The dispersion curve of the


 FIG. 11. MOR dispersion in neutron-irradiated CaO crystals (from^{32a}).

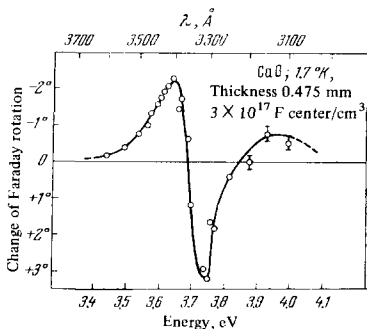
double resonance effect, $\Delta\Phi(\omega)$, shown in Fig. 12, makes it possible to determine immediately the position of the maximum of the absorption F band in CaO, namely 3.73 ± 0.06 eV. Relation (21) makes it possible to estimate the spin-orbit splitting parameter Δ . If we write the relation in a different form, noting (see Ch. I, Sec. 3) that $\alpha^{(0)} \sim Nf(n^2 + 2)^2/9n$, where N is the number of F centers per cubic centimeter and f is the oscillator strength of the transition, then we get at sufficiently low temperatures

$$\Phi_{\min} \approx \frac{2\pi^3}{3n} \left(\frac{n^2 + 2}{3} \right)^2 \left(\frac{l}{\lambda} \right) \left(\frac{Ne^2f}{m\omega_0} \right) \left(\frac{\Delta}{\delta_{1/2}} \right) \left(\frac{\Delta}{W} \right) \text{th} \left(\frac{\beta H}{kT} \right), \quad (52)$$

where $W = \hbar\omega_0$ is the center of gravity of the band, $\lambda = 2\pi c/\omega_0$, and l is the thickness of the sample. For the samples investigated in^[32a], $N = 3 \times 10^{17} \text{ cm}^{-3}$, $\lambda = 3300 \text{ \AA}$, $l = 0.5 \text{ mm}$, $n = 2.2$, and $H = 11 \text{ kG}$. The observed value $\Phi_{\min} = 2^\circ$ yields for $f\Delta$ a value 55 cm^{-1} . Putting $f \approx 0.8$, we get $\Delta \approx 70 \text{ cm}^{-1}$, which amounts to only one-third of the value $\Delta = 225 \text{ cm}^{-1}$ for the free Ca^+ ion. For MgO we have $\Delta \approx 30 \text{ cm}^{-1}$.

It was shown in^[32b] as a result of a MOR investigation that the narrow 3557 \AA line on the long-wave edge of the F band in CaO is a phononless line due to a purely electronic transition in the F center. In addition, certain simple details of the dispersion curve of the magneto-optic rotation in the F-band region were established. The spin-orbit splitting parameter Δ was determined in this case by the method of moments (formula (41)): $\Delta = -(80 \pm 10) \text{ cm}^{-1}$, which agrees within the limits of the calculation accuracy with the value $\Delta = -70 \text{ cm}^{-1}$ given above.

MOR investigations^[111] have made it possible to identify the optical absorption band belonging to F centers in SrO and BaO, and to measure the values of


 FIG. 12. Dispersion of double resonance in CaO crystals with color centers ($T = 1.7^\circ \text{ K}$) (from^[32a]).

the spin-moment interaction constants $\lambda' = 2\Delta/3$ in CaO, SrO, and BaO. The measurements were made of samples irradiated with neutrons and protons (maximum optical density ~ 2). The absorption F bands in SrO and BaO lie near 3 and 2 eV respectively. The spin-orbit interaction constants λ' were determined on the basis of MOR data with the aid of the method of moments, and turned out to equal -24 cm^{-1} , -185 cm^{-1} , and -265 cm^{-1} for CaO, SrO, and BaO respectively. We note that the value $\lambda' = -24 \text{ cm}^{-1}$ deviates greatly from the data of^[32], according to which $\lambda' = -50 \text{ cm}^{-1}$. The causes of this discrepancy are still not clear.

3. Rare-earth Activator Centers

As is well known, the most characteristic feature of rare-earth activator centers is the presence of an incomplete 4f shell, which is sufficiently well screened from the influence of the nearest surrounding. The parity-forbidden optical transitions between the levels of the configuration $4f^k$ correspond to narrow absorption and emission bands, which can be investigated by the Zeeman-spectroscopy or with the aid of the piezo-spectroscopic effect^[62]. The Faraday effect in the region of these narrow absorption bands was investigated by H. Becquerel et al.*, but these investigations were not pursued further, since the information obtained in such cases does not differ essentially from that extracted from investigations of the Zeeman splitting. It is known, however, that besides the forbidden f-f transitions, there can be observed in the optical spectra of the ions of the rare-earth series also parity-allowed transitions in mixed configurations, for example for $4f^{k-1}5d$, which appear in the form of broad intense bands in the absorption and luminescence spectra^[63].

In the case of trivalent rare-earth ions, the greater part of the terms of the mixed configurations lie in the far ultraviolet region of the spectrum, where the number of transparent bases is limited, as a result of which these terms have not been investigated in detail.^[64] Some exceptions are the Ce^{3+} and Yb^{3+} ions, whose mixed-configuration levels lie relatively low.

Allowed f-d transitions are extensively represented in the spectra of divalent rare-earth ions, which are characterized by a relatively low location of the energy levels of the mixed configurations^[63,65]. Broad intense absorption bands are observed in this case not only in the UV region, but also in the visible and IR regions. The large width of the bands excludes the possibility of obtaining suitable information with the aid of spectroscopic research methods in external fields, with the exception of the MOR and MCD methods.

In recent years, MOR and MCD investigations in the region of dipole interconfiguration transitions were performed for a number of doubly and triply charged ions in cubic crystals of alkali-earth fluorides (MeF_2) having the structure of fluorite^[66,75]. We mention here only the most characteristic examples of such investigations that have been interpreted by now to some degree.

a) Systems with even numbers of electrons. The

*The results of these investigations are given in [2].

ground state in the cubic crystal field is as a rule an orbital singlet, as a result of which there is no paramagnetic rotation. The MOR and MCD effects are due in this case either to magnetic splitting of the energy levels of the excited states (diamagnetic MOR and MCD), or to a redistribution of the intensities of the σ_+ and σ_- transitions under the influence of the magnetic field.

By way of an example let us consider the samarium ion in a fluorite crystal ($\text{CaF}_2\text{-Sm}^{2+}$, configuration $4f^6$, lower level of ground state 7F_0 —orbital singlet $^1\Gamma_1$). For this system, the MCD dispersion was investigated in the region of narrow lines on the long-wave edge of the absorption band I (650–600 nm)^[68] and the MOR dispersion in the region of the absorption band II ($\lambda_{\text{max}} = 426 \text{ nm}$)^[69]. An investigation of the MCD dispersion was made for two purposes: 1) to test the procedure, by redetermining the g-factors of the levels 263 and 14497 cm^{-1} , which were previously obtained by another method and which are equal to 1.3 and 0.39, respectively, and 2) to measure the g-factors of other levels, which cannot be obtained with the aid of the standard technique by virtue of the appreciable width of the corresponding absorption lines. It was established empirically that the observed MCD dispersion curve in the region of each line is described by the relation

$$k_H^{\sigma_+, \nu} - k_H^{\sigma_-, \nu} = Ak_0^{\sigma\nu} - 2\beta gH \frac{dk_0^{\sigma\nu}}{d\nu}, \quad (53)$$

where $k_0^{\sigma\nu}$ is the absorption coefficient in the absence of the field. The coefficient A characterizes the difference between the observed MCD curve and the $dk^{\sigma\nu}/d\nu$ curve. This method was used to find the g-factors and the coefficients A for a number of levels^[68]. The MOR dispersion curve in the region of band II (Fig. 13)^[69] is apparently a superposition of two S-shaped curves which have opposite rotation signs at the maxima. By calculating the relative intensities of the σ_{\pm} components it can be shown that the isolated pair of states effectively influencing one another in the presence of a magnetic field, produces opposite signs of the Faraday rotation in the corresponding pairs of transitions^[70].

An analogous investigation of the MOR dispersion was carried out for the ion Yb^{2+} in fluorite (configuration $4f^{14}$, ground state $^1S_0(^1\Gamma_1)$ in the region of the 365 nm absorption band ($T = 300^\circ\text{K}$, $H = 10 \text{ kOe}$), where the

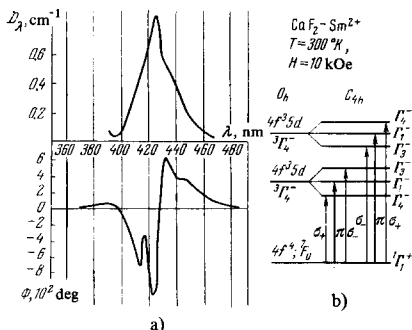


FIG. 13. a) Absorption spectrum (top) and MOR dispersion (bottom) in $\text{CaF}_2\text{-Sm}^{2+}$ crystals ($T = 300^\circ\text{K}$, $H = 10 \text{ kOe}$). b) Energy level scheme of Sm^{2+} in a cubic crystal field (symmetry O_h) and in a magnetic field (symmetry C_{4h}) (from [69]).

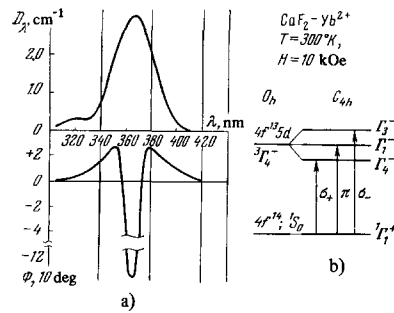


FIG. 14. a) Absorption spectrum (top) and MOR dispersion (bottom) in $\text{CaF}_2\text{-Yb}^{2+}$ crystals ($T = 300^\circ\text{K}$, $H = 10 \text{ kOe}$). b) Energy level scheme of Yb^{2+} in a cubic crystal field (symmetry O_h) and in a magnetic field (symmetry C_{4h}) (from [69]).

rotation is predominantly diamagnetic (Fig. 14), and for the Dy^{2+} ion (configuration $4f^{10}$, ground state $^5I_8(^2\Gamma_3)$) in the region 400–700 nm, where the rotation is determined mainly by the redistribution of the intensities of the σ_+ and σ_- components in the region of the f–d transitions^[69,70].

b) Systems with an numbers of electrons. In this case the ground state in the cubic crystal field is as a rule a Kramers doublet, as a result of which the MOR and MCD exhibit a temperature dependence characteristic of paramagnetism. From the form of the dispersion curves of the paramagnetic MOR and MCD it is possible to assess directly the predominance of one of the σ components in the transition. If, in addition, the symmetry of the lower level is known (from EPR data) then, by determining theoretically (or from results of an investigation of the Zeeman effect on the f–f transitions) the location of its magnetic sublevels, and by using the selection rules with allowance for the relative intensities of the σ_+ and σ_- transitions (which are obtained theoretically), it is possible to establish the symmetry of the second level that takes part in the optical transition. A similar investigation, carried out over the entire spectral interval, makes it possible to construct the mixed-configuration energy-level scheme and to arrange them on the energy scale (in the presence of theoretical predictions) by comparing the levels of equal symmetry.

Such level schemes were constructed for the ions Ho^{2+} ^[71], Tu^{2+} ^[71,72], Ce^{3+} ^[73], and also U^{3+} ^[74] in crystals of the fluorite type (MeF_2). By way of an example, Fig. 15 shows the absorption spectra, the MOR dispersion curves, and the energy level scheme of the mixed configurations of the ion Tu^{2+} , established by the method described above on the basis of an analysis of the MOR^[71] and MCD^[72] data. Analogous data are shown in Fig. 16 for trigonal activator centers in $\text{CaF}_2\text{-Ca}^{3+}$ crystals, and in Fig. 17 for U^{3+} ions in CaF_2 ^[74].

Another method of analyzing data on the Faraday rotation in fluorite crystals activated with divalent europium ($\text{CaF}_2\text{-Eu}^{2+}$) was proposed in^[26,75]. For free ions in the S-state, electric dipole transitions are allowed to the states of the type $P: S \rightarrow P_{J-1}, P_J, P_{J+1}$. If the frequency of the incident light is sufficiently remote from all the levels of the P_J multiplet (is located far beyond its limits), then the rotation is proportional,

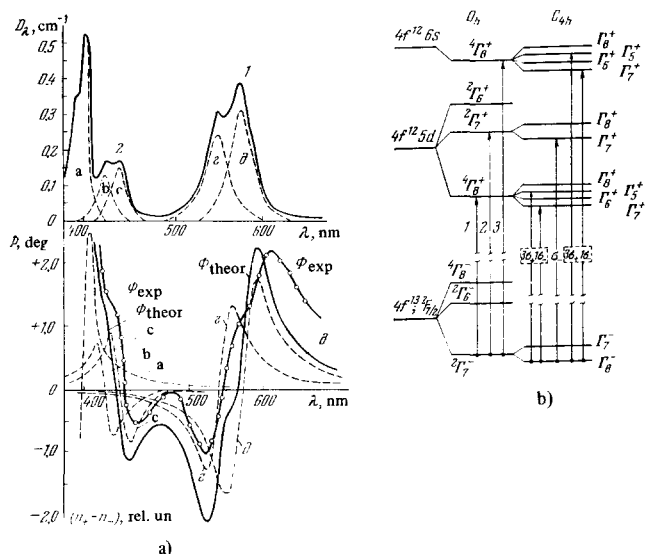


FIG. 15. Absorption spectrum (top) and MOR dispersion (bottom) in $\text{CaF}_2\text{-Tu}^{2+}$ crystals ($T = 4.2^\circ \text{K}$, $H = 13 \text{ kOe}$). The dashed lines indicate the resolution into elementary absorption bands and their contribution to the MOR. Φ_{theor} —summary dispersion curve, Φ_{exp} —experimental curve. b) Energy level scheme of Tu^{2+} ion in a cubic crystal field (O_h) and the level splitting following application of a magnetic field (C_{4h}) (from [71]).

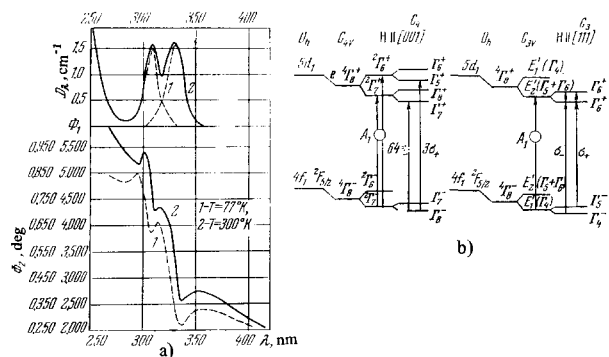


FIG. 16. a) Absorption spectrum (top) and MOR dispersion (bottom) in $\text{CaF}_2\text{-Ca}^{3+}$ crystals ($T = 77^\circ$ and 300°K). b) Energy level scheme of the ion (tetragonal and trigonal centers) in magnetic fields (from [73]).

with good accuracy, to the mean value of the orbital-angular momentum projection $\langle L_Z \rangle$, and consequently is vanishingly small for ions in the ground S state [3]. This was experimentally confirmed for the ions Gd^{3+} [77] and Mn^{2+} [78]. The small residual paramagnetic rotation is in this case proportional to the magnetization. When the light frequency is close to one of the Pj levels, but does not fall into the region of its Zeeman structure, the rotation for ions in the ground S state can be quite large, but still proportional to the magnetization. This reasoning can be employed in some cases also for interstitial S-state ions in crystals. Indeed, in a cubic crystal field, the Stark splitting of the Pj levels is very small ($\sim 10 \text{ cm}^{-1}$), since the cubic crystal field splits the P term only in higher orders of perturbation theory in conjunction with the spin-orbit interaction [79]. The quantum number J is there-

fore sufficiently good. A similar situation is realized apparently for Eu^{2+} ions in fluorite (which have, like the isoelectronic Gd^{3+} , a ground state $^8S_{7/2}$, where an appreciable Faraday rotation, proportional to the magnetization, was observed [75] in the visible region. The rotation in the visible region for divalent rare-earth ions in crystals of the fluorite type is due to dipole interconfiguration transitions $(4f)^7 \rightarrow (4f)^6(5d)$ for Eu^{2+} . The foregoing reasoning shows that in this case the electric-dipole transitions is realized in a state of the Pj type ($P_{5/2}$, $P_{7/2}$, $P_{9/2}$). The MOR dispersion was investigated also in [75] in the region of narrow absorption lines: the 4130 Å lines of Eu^{2+} in CaF_2 (at low europium concentrations), located on the long-wave edge of the f-d transition region, and the four narrow lines of Nd^{3+} in CaF_2 , corresponding to the interconfiguration $(4f)^3 \rightarrow (4f)^2(5d)$ transitions. The MOR dispersion has in these cases a characteristic S-shape (regular or inverted, of the type shown in Figs. 2, II, d and e). The experimentally obtained values of Φ_{max} in the region of the four lines of Nd^{3+} in CaF_2 were used to verify relations of the type (32), which give the connection between the rotation, circular dichroism, and the line width (for lines with a Lorentz shape). The agreement between the calculated and experimentally obtained values of Φ_{max} is satisfactory.

In [80], using anisotropic activator centers in $\text{CaF}_2\text{-Cu}^{3+}$ and $\text{BaF}_2\text{-U}^{3+}$ as examples, it was shown that measurement of the MOR and MCD can be used together with other methods [81] to determine the orientation of the anisotropic activator centers in a cubic crystal lattice (to reveal the "latent optical anisotropy"). The methods based on an investigation of the circular anisotropy are in this case more universal than the others with respect to the choice of objects, since they can be successfully used for the study of nonluminescent centers with broad bands. The data obtained for the crystals $\text{CaF}_2\text{-Ca}^{3+}$ indicated, in agreement with the data obtained by other methods, that the centers responsible for the absorption band with maximum near 305 nm have tetragonal symmetry.

An investigation of MOR far from the absorption bands due to the dipole interconfiguration transitions

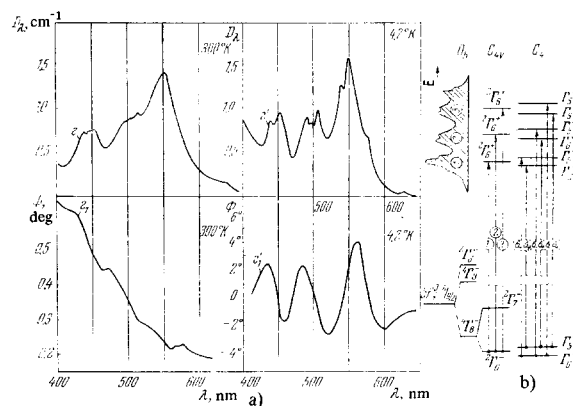


FIG. 17. a) Absorption spectra (top) and MOR dispersion (bottom) in $\text{CaF}_2\text{-U}^{3+}$ crystals ($T = 4.2$ and 300°K). b) Energy level scheme of the U^{3+} ion in a tetragonal crystalline field. (Symmetry C_{4v}) and their splittings following application of a magnetic field along the tetragonal axis (symmetry C_4) (from [74]).

was made with yttrium-aluminum garnet crystals activated with erbium ($\text{Y}_3\text{Al}_5\text{O}_{12}\text{-Er}^{3+}$) as an example^[82]. The dependence of Φ on the wavelength of the light is described by the relation (20) or $W = (62 \pm 4) \times 10^{-3} \text{ cm}^{-1}$. Thus, the energy of the lowest term of the excited mixed configuration of the Er^{3+} has been established, and agrees within the limits of the specified accuracy with the energy of the lowest $4f \rightarrow 5d$ transition ($64.2 \times 10^3 \text{ cm}^{-1}$ according to the data of^[64]) in the Er^{3+} ion (configuration $4f^{11}$, ground term $^4I_{15/2}$).

The influence of a microwave electromagnetic field on the Faraday rotation in a constant magnetic field was investigated in^[83], where it was shown that a combination of the action of these fields expands the methodological capabilities of the EPR method, making it possible to investigate the saturation of spin systems by means of optical observations. The authors observed in $\text{CaF}_2\text{-Eu}^{2+}$ crystals the saturation of the sublevels of the ground state of the Eu^{2+} ion ($^8S_{7/2}$) and determined their g-factors.

4. Complexes of Transition Metals with Incomplete d Shells

The absorption bands of complexes of transition metals located in the visible and near UV regions are due, as a rule, to transitions within the incomplete d shell. The intensities of these transitions depend on the nature and on the geometrical configuration of the ligands surrounding the central ion, and are usually small, since the corresponding transitions are parity-forbidden in first approximation. For octahedral complexes, the absorption in the visible region is apparently connected with the odd vibrational modes of the ligands, which disturb the symmetry center; the oscillator strengths of the transitions are in this case $f \approx 10^{-4} - 10^{-5}$ ^[84]. For tetrahedral complexes, $f \approx 10^{-3}$. Such a relatively strong absorption, according to^[84], can be due to the following: 1) mixing of 3d and 4p orbitals in a tetrahedral crystalline field and 2) mixing of 3d orbitals and of the wave functions of the ligands (covalence effects). This shows that the crystal-field theory is insufficient to explain the intensities in the absorption of such complexes, and calls for further development. MOR investigations have recently come into use for the determination of the limits of applicability of the crystal-field theory in complexes of transition metals^[85-88]. In particular, the Faraday rotation of the tetrahedral complex CoCl_4^{2-} was investigated theoretically in^[87] on the basis of the theory of the crystalline field. Satisfactory agreement between the calculated and measured^[89] values of the Verdet constants at individual frequencies (near the maximum of the absorption band $\sim 14500 \text{ cm}^{-1}$) was obtained. It was therefore concluded that the MOR can be satisfactorily described within the framework of the crystal-field theory, in spite of the fact that it encounters the aforementioned difficulties when it comes to explaining the intensities in the absorption of such complexes and when attempts are made to explain the natural optical activity^[90].

A critical analysis of investigations of this kind was presented in^[87] on the basis of the notions developed in Sec. 3 of Ch. I. The transition $^4A_2 \rightarrow ^4T_1(P)$, re-

sponsible for the 14500 cm^{-1} absorption band of the CoCl_4^{2-} complex, is considered. The wave functions of the corresponding states are written in the approximation of the weak crystal field^[87], with no limitations imposed on the nature of the e and t_2 orbitals, making it possible to consider simultaneously two variants of the theory: 1) the theory of the crystal field, when the t_2 orbitals are a mixture of d and p orbitals of the central line, and 2) a variant of the molecular-orbital method^[91], when the e and t_2 orbitals are a mixture of d orbitals of the central ion and the wave functions of the ligands. In the limits when the spin-orbit interaction can be neglected, the parameter C in formula (33), which determines the fraction of the paramagnetic rotation, is equal to zero. The parameters A and B, which determine diffraction of the diamagnetic rotation and the rotation due to the "mixing" of the states, are calculated: 1) within the framework of the crystal-field theory:

$$\frac{A}{D} = 0.33, \quad \frac{B}{D} = -\frac{1.67}{\Delta E}, \quad \frac{A}{B} = -0.2\Delta E. \quad (54)$$

where $\Delta E = 3500 \text{ cm}^{-1}$ and D is the oscillator strength of the transition $^4A_2 \rightarrow ^4T_1(P)$:

2) within the framework of the simplest variant of the MO method:

$$\frac{A}{D} = 0.18, \quad -\frac{0.97}{\Delta E} < \frac{B}{D} < \frac{0.14}{\Delta E}, \quad -0.18\Delta E < \frac{A}{B} < 1.31\Delta E. \quad (55)$$

Thus

$$\frac{A_{\text{MO}}}{A_{\text{cr.f.}}} = 0.53, \quad -0.08 < \frac{B_{\text{MO}}}{B_{\text{cr.f.}}} < 0.58. \quad (56)$$

In principle, relations (54)–(56) provide a rather precise criterion for the applicability of either of the treatments. However, at the present time one can only estimate the contributions of the terms A and B, using the ratio of the maxima of the corresponding dispersion curves $9A/4\Gamma B$ (see Table I), and also $\Gamma \sim 2000 \text{ cm}^{-1}$ and the relation (45). As a result, $9A/4\Gamma B \approx 0.79$, i.e., the contributions of the terms A and B are comparable at the maximum of the band. In determining the Verdet constant at the 14390 cm^{-1} frequency it is therefore not permissible to neglect the contribution of the term A, as was done in^[87]. In this connection, the conclusion that the crystal-field theory is applicable for the description of the MOR of CoCl_4^{2-} complexes can apparently not be regarded as sufficiently well founded.

Mention should be made of a group of investigations of the Faraday rotation in magnetically centered crystals—ferrimagnetic garnets with structure $\text{Y}_3\text{Fe}_2(\text{FeO}_4)_3$, where the yttrium can be replaced by different ions of the rare-earth series, for example Gd, Dy, Tb, and Ho. The rotation of the plane of polarization observed in this case is, generally speaking, not the Faraday effect in its usual sense. In magnetically concentrated crystals, the magnetic field is produced more readily by exchange forces inside the medium, rather than by external forces. The external magnetic field in this case only orders the exchange fields, acting on individual electrons, or in other words, destroys the domain wall^[99].

Ferrimagnetic garnets have intense optical absorption, the long-wave edge of which is located near

$\lambda \sim 1 \mu$. The Faraday effect in the near IR, sufficiently remote from the absorption edge, $\lambda > 4 \mu$, was investigated in a number of studies^[94-101]. It was shown that in this region the MOR is due to the precession of the magnetic moments of the ferrite sublattices under the influence of the magnetic field of the light wave, i.e., it is a consequence of magnetic resonance^[94,95,96]. In this case an investigation of MOR can be used to determine the Lande g-factors of the ions taking part in the ferrimagnetism.

The Faraday effect in the region of the edge of the absorption band of ferrimagnetic garnets was also investigated experimentally^[92] and theoretically^[93]. It is connected with the optical transition ${}^6S \rightarrow {}^4T_1$ (4G) in the Fe^{3+} ion (configuration $3d^5$), which is in the electric crystal field of octahedral symmetry and in a strong exchange field. In the first approximation, the transition is parity forbidden ($f \sim 10^{-9}$), but it becomes much stronger owing to an admixture of states of opposite parity ${}^6P(3d^4p)$ resulting from electron-phonon interaction ($f \sim 10^{-4}-10^{-5}$). If it is assumed that the corresponding absorption band has a Gaussian shape (15), then, taking the ratio of the maximum polarization-plane rotation angle (21) to the absorption coefficient at the center of the band, we get $\Phi_{max}/\alpha^{(0)} = 0.013$. Experiment yields 0.008. The order-of-magnitude agreement is evidence that the developed theory is not contradictory.

The Faraday effect in yttrium and holmium iron garnets was investigated in^[112,113] in strong pulsed magnetic fields (up to 160 kOe) in the visible region of the spectrum (in the vicinity of 6000 Å). In rare-earth iron garnets, the MOR can be regarded as a sum of independent contributions of all the ferrite sublattices. The MOR of the Fe^{3+} ions in the ground S state, at a fixed temperature and magnetic field intensity, will be proportional to the projection of their magnetization on the light propagation direction*. The MOR of the rare-earth sublattice is of opposite sign and of different magnitude than the resultant MOR of the iron-ion sublattices, at the same direction of their magnetizations. This means that there is no compensation of the MOR but there is compensation of the magnetic moments at the point T_c (magnetic compensation temperature). On going through T_c , an abrupt reversal of the sign of the MOR is observed, due to the turning (changing of the directions of the vectors) of the magnetic moments in sufficiently strong magnetic fields. Investigation of these processes by the MOR method makes it possible to obtain additional information on the sublattice motion; this information is usually obtained by measuring the total magnetic moment^[94].

The same method was used to investigate the MOR in the antiferromagnetic crystals MnF_2 and $RbMnF_3$ ^[114]. The MOR dispersion in the visible region can be approximately represented in the form of a

sum of two terms: a quadratic term dependent on the frequency (formula (20) with $W \gg E$), due to the absorption of light in the region of the maximum ultraviolet, and a frequency-independent term that varies with the temperature (formula (20) with $E \gg W$), due to the magnetic-dipole transitions in the microwave region of the spectrum (antiferromagnetic resonance). The appreciable change of the coefficient of proportionality between the rotation that is quadratically dependent on the frequency, and the magnetization (by a factor of almost 5 in the MnF_2 crystal) in the process of antiferromagnetic ordering (upon cooling below the Neel point) indicates that appreciable changes take place during antiferromagnetic ordering in the excited state that takes part in the high-energy optical transition. This circumstance, in particular, does not make it possible to connect this transition with the ${}^6S_6(3d^5) \rightarrow {}^6P(3d^4p)$ transition within the individual manganese ion.

MOR was also used to investigate the long-wave absorption edge in ferromagnetic crystals (halides of chromium ($CrCl_3$, $CrBr_3$, and CrI_3)^[115], due to the charge transport from the halide ion to the Cr^{3+} ion. The MOR data were interpreted within the framework of the concept of transitions within a complex that includes the $Cr^{3+}(3d^3)$ ion and the six halide ions surrounding it. On the basis of the MOR data it was possible to determine the electron configuration of the excited state (in terms of the molecular orbitals) and to explain the tremendous rotation (50000 deg/cm) that is characteristic of these compounds.

IV. CONCLUSIONS

We have described above certain method of investigating the energy structure of crystals on the basis of the dispersion investigations of the characteristics of the light (linearly or circularly polarized) passing through a material medium along an external static magnetic field. It can be seen that these investigations, which have been excessively developed in recent years, make it possible to extract considerable information which is inaccessible to other methods. We can now attempt to indicate certain possible trends for further development of research of this type.

First, it becomes possible to employ measurements of the degree of circular polarization of luminescence to investigate the energy structure of solids^[42,69]. By way of an example, we can consider the simplest energy-level scheme shown in Fig. 2, I. In the presence of an external static magnetic field, under conditions of thermal equilibrium, it becomes possible to observe a definite degree of circular polarization of the luminescence connected with transitions from the upper magnetic sublevels (by virtue of the difference between the populations of the upper sublevels at sufficiently low temperatures). Such an "inverse paramagnetic effect of MCD" can be regarded as an optical supplement to EPR investigations under conditions of overpopulation of the upper states. There are still no reliable experimental data on the observation of such phenomena.

We can indicate also another possible trend of the magneto-optical methods, in which an external static

*It should be borne in mind that in this case the temperature dependence of the MOR is rather complicated, in view of the fact that the investigated spectral region is adjacent, on the short-wave side, to the intrinsic absorption edge at 20000 cm^{-1} , and is adjacent on the long-wave side to the broad intense absorption bands at 11000 and 16400 cm^{-1} ^[92].

magnetic field is dispensed with, namely search for magneto-optical effects in optical-frequency fields. At the present time there is a known corresponding electro-optical analog^[102], where the birefringence effect is used for the registration of small Stark splittings of levels in electric fields of optical frequency. We can expect analogously small Zeeman splittings of degenerate levels under the influence of the magnetic component of a powerful high-frequency electromagnetic field, corresponding to the region of the magnetic dipole transitions including the considered degenerate level. To register these splittings one can apparently use effects of depolarization of the reference light. It should be noted, however, that the effects expected in this case have no direct bearing on the traditional MOR and MCD described above.

Mention can also be made of the so-called "inverse Faraday effect," observed recently in a number of investigations. The gist of this phenomenon is that transitions connected with the change of the magnetic moment of the system are effected in the medium under the influence of a strong circularly-polarized light flux. These changes are revealed by a current pulse which is produced in the circuit in which the medium is connected.

The inverse Faraday effect was observed in a ruby crystal under the influence of circularly-polarized radiation from a Q-switched ruby laser^[103]. A current pulse was produced in a coil surrounding the crystal target, and the magnitude of the pulse offered evidence that up to 20% of the chromium ions in the ruby changed their spin state. An analysis of the pulse has made it possible to estimate the spin-lattice relaxation time, which turned out to be 10^{-7} sec at room temperature.

Unlike this case, where the spin inversion was the result of a transition of ions into real states, the inverse Faraday effect was observed in^[104] in the region of transparency of the investigated media, i.e., in excitation of virtual states. This phenomenon was investigated in optical glasses, in certain organic and inorganic liquids, and in fluorite crystals activated with divalent europium ($\text{CaF}_2\text{-Eu}^{2+}$), which are transparent to the radiation of the employed ruby laser. The theory of the inverse Faraday effect is presented in^[105].

¹A. Righi, *Nuovo Cimento* (3), 3, 312 (1878); H. Becquerel, *Compt. Rend.* 88, 334 (1879).

²W. Schütz, *Magneto-optik*, Hdb. d. Experimentalphysik, Bd. 16, Akad. Verlag, Leipzig, 1936.

³L. Rosenfeld, *Zs. Phys.* 57, 835 (1930).

⁴R. de L. Kronig, *Zs. Phys.* 45, 458, 508 (1927).

⁵H. A. Kramers, *Proc. Acad. Sci. Amsterdam* 33, 959 (1930).

⁶R. Serber, *Phys. Rev.* 41, 489 (1932).

⁷J. T. Hougén, *J. Chem. Phys.* 32, 1122 (1960).

⁸T. Carrol, *Phys. Rev.* 52, 822 (1937).

⁹A. D. Buckingham and P. J. Stephens, *Annual Rev. Phys. Chem.* 17, 399 (1966).

¹⁰E. D. Palik and B. W. Hennis, *Appl. Opt.* 6, 603 (1967).

¹¹R. de L. Kronig, *J. Opt. Soc. Am.* 12, 547 (1926).

¹²H. A. Kramers, *Atti del Congresso Intern. dei*

Fisici 2, 545 (1928).

¹³E. Stern, *Solid State Phys.* 15, 299 (1963).

¹⁴I. M. Boswarva, R. E. Howard, and A. B. Lidiard, *Proc. Roy. Soc.* A269, 125 (1962).

¹⁵F. C. Brown and G. Laramore, *Appl. Opt.* 6, 669 (1967).

¹⁶L. D. Landau and E. M. Lifshits, *Élektrodinamika sploshnykh sred*, Gostekhizdat, 1959 (Electrodynamics of Continuous Media, Addison-Wesley, 1960).

¹⁷C. Djerassi, *Optical Rotatory Dispersion*, Ch. 12, McGraw-Hill, 1960.

¹⁸J. Mort, F. Lüty, and F. Brown, *Phys. Rev.* 137, A566 (1965); Yu. E. Perlin and L. S. Kharchenko, *Uch. Zap. (Science Notes) Kishinev Univ. Phys. Ser.* 90, 3 (1967).

¹⁹W. L. Miller and A. R. Gordon, *J. Phys. Chem.* 35, 2785 (1931).

²⁰I. B. Rosser, *Theory and Application of* $\int_0^z e^{-x^2} dx$ and $\int_0^z e^{-p^2 y^2} dy \int_0^y e^{-x^2} dx$, 1948.

²¹A. M. Clogston, *J. Phys. et Radium* 20, 151 (1959).

²²C. H. Henry, S. E. Schnatterly, and C. P. Slichter, *Phys. Rev.* 137, 583 (1965).

²³C. H. Henry, *Phys. Rev.* 140, 256 (1965).

²⁴F. Brown, B. C. Cavenett, and W. Hayes, *Proc. Roy. Soc.* A300, 78 (1967).

²⁵M. Lax, *J. Chem. Phys.* 20, 1752 (1952).

²⁶Y. R. Shen, *Phys. Rev.* 133, A511 (1964).

²⁷H. Eyring et al., *Quantum Chemistry*, Wiley, 1944.

²⁸L. Velluz, et al., *Optical Circular Dichroism*, Academic 1965; F. Woldbye, in *Optical Rotatory Dispersion and Circular Dichroism in Org. Chemistry*, Ed. by G. Sznatzke, Heyden a. Son, 1967; p. 85.

²⁹N. A. Tolstoj and P. P. Feofilov, *Dokl. Akad. Nauk SSSR* 60, 219 (1948).

³⁰N. V. Karlov, J. Margerie, Y. Merle d'Aubigne, *J. de Phys. et Radium* 24, 717 (1963).

³¹R. Onaka, T. Mabushi, and A. Yoshikawa, *J. Phys. Soc. Japan* 23, 1036 (1967).

^{32a}J. C. Kemp, W. M. Ziniker, and J. A. Glaze, *Proc. Brit. Ceram. Soc.* 9, 109, (1967); J. C. Kemp, W. M. Ziniker, J. A. Glaze, and J. C. Cheng, *Phys. Rev.* 171, 1024 (1968).

³³M. V. Vol'kenshteĭn, Yu. A. Sharonov, i dr., *Molekulyarnaya Biologiya* 1, 467, 476 (1967); *Nature* 209, 709 (1966).

³⁴J. Badoz, B. Briat, and M. Billardon, *Japan. J. of Appl. Phys.* 4, Suppl. 1, 600 (1965); M. Billardon, and J. Badoz, *Compt. Rend.* 263, 139 (1966), A.-C. Boccara, O. Roubeau, and J. Badoz, *Compt. Rend.* 265, 513 (1967).

³⁵J. G. Forsythe, R. Kieselbach, and V. E. Shashoua, *Appl. Opt.* 6, 699 (1967).

³⁶Yu. A. Sharonov, *Opt. Spektrosk.* 25, 930 (1968).

³⁷D. L. Dexter, *Phys. Rev.* 111, 119 (1958).

³⁸F. Lüty, and J. Mort, *Phys. Rev. Lett.* 12, 45 (1964).

³⁹R. Romestain and J. Margerie, *Compt. Rend.* 158, 2525 (1964).

⁴⁰J. Margerie and R. Romestain, *Compt. Rend.* 258, 4490 (1964).

⁴¹J. H. Rabin and J. H. Schulman, *Phys. Rev.* 125, 1584 (1962); D. W. Lynch, *Phys. Rev.* 127, 1537 (1962); M. Suffczynski, *J. Chem. Phys.* 38, 1558 (1963); R. S.

- Knox, *Phys. Rev.* **133**, A 498 (1964); D. B. Fitchen, *Phys. Rev.* **134**, A 1599 (1964).
- ⁴²J. Margerie, Les centres colorés dans les cristaux ioniques, *J. de Phys.*, Coll. C4, suppl. au n° 8-9 (1967), p. 103.
- ⁴³Y. Merle d'Aubigné, and J. Gareyte, *Compt. Rend.* **261**, 689 (1965).
- ⁴⁴F. C. Brown, B. C. Cavenett, and W. Hayes, *Phys. Lett.* **19**, 167 (1965).
- ⁴⁵E. Krätzig and W. Staude, *Phys. Lett.* **26A**, 133 (1968).
- ⁴⁶G. Gehrler and H. Langer, *Phys. Lett.* **26A**, 232 (1968).
- ⁴⁷H. Härtel and F. Lüty, *Zs. Phys.* **182**, 111 (1964).
- ⁴⁸P. Duval, J. Gareyte, and Y. Merle d'Aubigné, *Phys. Lett.* **22**, 67 (1966); Y. Merle d'Aubigné, P. Duval, Les centres colorés dans les cristaux ioniques, *J. de phys.*, Suppl. au n° 8-9 (1967), p. 112.
- ⁴⁹R. H. Silsbee, *Phys. Rev.*, **138**, 181 (1965).
- ⁵⁰I. W. Shepherd, *Phys. Rev.* **165**, 985 (1968).
- ⁵¹C. J. Delbecq, W. Hayes, M. C. O'Brien, and P. H. Yuster, *Proc. Roy. Soc.* **A271**, 243 (1963).
- ⁵²J. Owen, *Proc. Roy. Soc.* **A227**, 183 (1965).
- ⁵³J. Arends, *Phys. stat. sol.* **7**, 805 (1964).
- ⁵⁴P. P. Feofilov, *Zh. Eksp. Teor. Fiz.* **26**, 609 (1954); G. A. Tishchenko and P. P. Feofilov, *Izv. AN SSSR, ser. fiz.* **20**, 482 (1956); P. Görlich, H. Karras, and R. Lehmann, *Phys. Stat. Sol.* **1**, 389, 525 (1961).
- ⁵⁵B. C. Cavenett, W. Hayes, and I. C. Hunter, *Solid State Comm.* **5**, 635 (1967).
- ⁵⁶M. S. Bennett and A. B. Lidiard, *Phys. Lett.* **18**, 253 (1965).
- ⁵⁷P. Feltham, *Phys. stat. sol.* **20**, 675 (1967).
- ⁵⁸J. E. Wertz, G. S. Saville, L. Hall, and P. Auzins, *Proc. Brit. Ceram. Soc.* (1), 59 (1964).
- ⁵⁹J. W. Culvathouse, L. V. Holoroyd, J. L. Kolopus, *Phys. Rev.* **140**, A1181 (1965); W. P. Unruh and J. W. Culvathouse, *Phys. Rev.* **154**, 861 (1967).
- ⁶⁰J. C. Kemp and V. I. Neely, *Phys. Rev.* **132**, 215 (1963).
- ⁶¹J. C. Kemp, W. M. Ziniker, and J. A. Glaze, *Phys. Lett.* **22**, 37 (1966).
- ⁶²B. P. Zakharchenya and A. A. Kaplyanskii, *Spektroskopiya kristallov (Trudy simposiuma) (Crystal Spectroscopy, Symposium Proceedings)*, Nauka, 1966, p. 99.
- ⁶³P. P. Feofilov, *Izv. AN SSSR, ser. fiz.* **26**, 435 (1962); *Acta phys. polon.* **26**, 331 (1965); *Spektroskopiya kristallov (Trudy simposiuma) (Crystal Spectroscopy, Symposium Proceedings)*, Nauka, 1966, p. 87.
- ⁶⁴E. Loh, *Phys. Rev.* **147**, 332 (1966); **154**, 270 (1967); **158**, 273 (1967).
- ⁶⁵Z. J. Kiss, *Phys. Rev.* **127**, 718 (1962); D. McClure and Z. J. Kiss, *J. Chem. Phys.* **39**, 3251 (1963).
- ⁶⁶Y. R. Shen, and N. Bloembergen, *Phys. Rev.* **133**, 515 (1964).
- ⁶⁷L. A. Alekseeva and P. P. Feofilov, *Opt. Spektrosk.* **22**, 996 (1967).
- ⁶⁸J. Margerie, *Physica* **33**, 238 (1967).
- ⁶⁹L. A. Alekseeva, N. V. Starostin, and P. P. Feofilov, *Spektroskopiya kristallov (Trudy 2-ogo simposiuma) (Crystal Spectroscopy, Proc. of 2nd Symposium)*, Nauka, 1969.
- ⁷⁰L. A. Alekseeva and N. V. Starostin, *Opt. Spektrosk.* **25**, 960 (1966).
- ⁷¹L. A. Alekseeva, N. V. Starostin, and P. P. Feofilov, *Opt. Spektrosk.* **23**, 259 (1967).
- ⁷²C. H. Anderson, H. A. Weakliem, and E. S. Sabisky, *Phys. Rev.* **143**, 223 (1966).
- ⁷³L. A. Alekseeva and N. V. Starostin, *Opt. Spektrosk.* **24**, 145 (1968).
- ⁷⁴L. A. Alekseeva, *Izv. AN Latv. SSSR, ser. fiz.-tekh.* **1**, 45 (1968).
- ⁷⁵Y. R. Shen, *Phys. Rev.* **134**, A661 (1964).
- ⁷⁶B. P. Zakharchenya and A. Ya. Ryskin, *Opt. Spektrosk.* **13**, 501 (1962).
- ⁷⁷J. Becquerel and J. van den Handel, *Physica* **7**, 711 (1940).
- ⁷⁸J. Becquerel, W. J. de Haas, and J. van den Handel, *Proc. Acad. Sci. Amsterdam* **34**, 1231 (1931).
- ⁷⁹J. H. Van Vlek and W. C. Penney, *Phil. Mag.* **17**, 961 (1934).
- ⁸⁰L. A. Alekseeva and P. P. Feofilov, *Fiz. Tverd. Tela* **10**, 1773 (1968) [*Sov. Phys.-Solid State* **10**, 1397 (1968)].
- ⁸¹P. P. Feofilov and A. A. Kaplyanskiĭ, *Usp. Fiz. Nauk* **76**, 201 (1962); [*Sov. Phys.-Usp.* **5**, 79 (1963)].
- ⁸²W. Y. Lung and J. R. Chamberlain, *Phys. Lett.* **27A**, 365 (1968).
- ⁸³Y. Hayashi, M. Fukui, and H. Yoshioka, *J. Phys. Soc. Japan* **23**, 312 (1967).
- ⁸⁴A. D. Liehr, and C. J. Ballhausen, *Phys. Rev.* **106**, 1161 (1957); C. J. Ballhausen and A. D. Liehr, *J. Mol. Spectry* **2**, 342 (1958).
- ⁸⁵M. J. Stephen, *Mol. Phys.* **1**, 301 (1958).
- ⁸⁶A. J. Stone, *Mol. Phys.* **4**, 225 (1961).
- ⁸⁷Sheng-Hsien Lin and H. Eyring, *J. Chem. Phys.* **42**, 1780 (1965).
- ⁸⁸P. J. Stephens, *J. Chem. Phys.* **43**, 4444 (1965).
- ⁸⁹S. S. Bhotanagar, A. N. Kapur, and P. L. Kapur, *J. Indian Chem. Soc.* **13**, 489 (1936).
- ⁹⁰W. Moffit, *J. Chem. Phys.* **25**, 1189 (1956); S. Sugano, *J. Chem. Phys.* **33**, 1883 (1960); T. S. Piper and A. Karipides, *Mol. Phys.* **5**, 475 (1962).
- ⁹¹C. J. Ballhausen, *Introduction to Ligand Field Theory*, McGraw-Hill, 1962.
- ⁹²J. F. Dillon, *Bull. Phys. Soc.* **2**, 238 (1957).
- ⁹³A. M. Clogston, *J. Phys. et Rad.* **20**, 151 (1959).
- ⁹⁴G. S. Krinchik and M. V. Chetkin, *Zh. Eksp. Teor. Fiz.* **40**, 729 (1961) [*Sov. Phys.-JETP* **13**, 509 (1961); **38**, 1643 (1960)] *Sov. Phys.-JETP* **11**, 1184 (1960); **41**, 673 (1961) [*Sov. Phys.-JETP* **14**, 485 (1962)].
- ⁹⁵M. V. Chetkin, *Fiz. Tverd. Tela* **6**, 3753 (1964) [*Sov. Phys.-Solid State* **6**, 3013 (1965)].
- ⁹⁶G. S. Krinchik and G. K. Tyutneva, *Izv. AN SSSR, ser. fiz.* **38**, 489 (1964).
- ⁹⁷M. V. Chetkin and A. N. Shalygin, *Zh. Eksp. Teor. Fiz.* **52**, 882 (1967) [*Sov. Phys.-JETP* **25**, 580 (1967)].
- ⁹⁸B. Johnson and R. Teble, *Proc. Phys. Soc. (London)* **87**, 935 (1966).
- ⁹⁹B. Johnson, *Brit. J. Appl. Phys.* **17**, 1441 (1966).
- ¹⁰⁰M. V. Chetkin and A. N. Shalygin, *J. Appl. Phys.* **39**, 561 (1968).
- ¹⁰¹R. W. Cooper, W. A. Crossbey, J. L. Page, and R. F. Pearson, *J. Appl. Phys.* **39**, 565 (1968).
- ¹⁰²A. M. Bonch-Bruevich and V. A. Khodovoi, *Usp. Fiz. Nauk* **93**, 71 (1967) [*Sov. Phys.-Usp.* **10**, 637 (1968)].

- ¹⁰³G. F. Hull, J. T. Smith, and A. F. Quesada, *Appl. Opt.* **4**, 1117 (1965).
- ¹⁰⁴J. P. van der Ziel, P. S. Pershan, and L. D. Malmstrom, *Phys. Rev. Lett.* **15**, 190 (1965).
- ¹⁰⁵P. S. Pershan, J. P. van der Ziel, and L. D. Malmstrom, *Phys. Rev.* **143**, 574 (1966).
- ¹⁰⁶H. Paul and F. Lüty, *Phys. Lett.* **20**, 57 (1968).
- ¹⁰⁷W. Burke, *Phys. Rev.* **172**, 886 (1968); W. Burke, S. E. Schnatterly, and W. D. Compton, *Bull. Am. Phys. Soc.* **11**, 245 (1966).
- ¹⁰⁸J. A. Davis and D. B. Flitchen, *Solid State Commun.* **6**, 505 (1968).
- ¹⁰⁹A. Yoshikawa and T. Mabushi, *J. Phys. Soc. Japan* **24**, 1405 (1968).
- ¹¹⁰Y. Toyosawa and M. Inoue, *J. Phys. Soc. Japan* **20**, 1289 (1965).
- ¹¹¹R. G. Bessent, B. C. Cavenett, and I. C. Hunter, *J. Phys. Chem. Solids*, **29**, 1523 (1968).
- ¹¹²N. F. Kharchenko, V. V. Eremenko, and L. I. Belyi, *Zh. Eksp. Teor. Fiz.* **53**, 1505 (1967) and **55**, 419 (1968) [*Sov. Phys.-JETP* **26**, 869 (1968) and **28**, 219 (1969)].
- ¹¹³N. F. Kharchenko, L. I. Belyi, and O. N. Tutakina, *Fiz. Tverd. Tela* **10**, 2819 (1968) [*Sov. Phys.-Solid* **10**, 2221 (1969)].
- ¹¹⁴N. F. Kharchenko and V. V. Eremenko, *Fiz. Tverd. Tela* **9**, 1655 (1967) and **10**, 1402 (1968) [*Sov. Phys.-Solid State* **9**, 1302 (1967) and **10**, 1112 (1968)].
- ¹¹⁵J. F. Dillon, J. H. Kamimura, and J. P. Remeika, *J. Phys. Chem. Solids* **27**, 1531 (1966).
- ¹¹⁶B. Lax and J. G. Mavroides, *Appl. Opt.* **6**, 647 (1967).

Translated by J. G. Adashko